



HAL
open science

Aleppo pine seeds (*Pinus halepensis* Mill.) as a promising novel green coagulant for the removal of Congo red dye: Optimization via machine learning algorithm

Amina Hadadi, Ali Imessaoudene, Jean-Claude Bollinger, Abdelkrim Bouzaza, Abdeltif Amrane, Hichem Tahraoui, Lotfi Mouni

► To cite this version:

Amina Hadadi, Ali Imessaoudene, Jean-Claude Bollinger, Abdelkrim Bouzaza, Abdeltif Amrane, et al.. Aleppo pine seeds (*Pinus halepensis* Mill.) as a promising novel green coagulant for the removal of Congo red dye: Optimization via machine learning algorithm. *Journal of Environmental Management*, 2023, 331, pp.117286. 10.1016/j.jenvman.2023.117286 . hal-03971845

HAL Id: hal-03971845

<https://hal.science/hal-03971845>

Submitted on 31 Mar 2023

HAL is a multi-disciplinary open access archive for the deposit and dissemination of scientific research documents, whether they are published or not. The documents may come from teaching and research institutions in France or abroad, or from public or private research centers.

L'archive ouverte pluridisciplinaire **HAL**, est destinée au dépôt et à la diffusion de documents scientifiques de niveau recherche, publiés ou non, émanant des établissements d'enseignement et de recherche français ou étrangers, des laboratoires publics ou privés.



Distributed under a Creative Commons Attribution - NonCommercial 4.0 International License

1 **Aleppo pine seeds (*Pinus halepensis* Mill.) as a promising novel**
2 **green coagulant for the removal of Congo red dye: optimization via**
3 **machine learning algorithm**

4 Amina Hadadi*¹, Ali Imessaoudene¹, Jean-Claude Bollinger², Abdelkrim Bouzaza³,
5 Abdeltif Amrane³, Hichem Tahraoui⁴, Lotfi Mouni¹

6
7 ¹Laboratoire de Gestion et Valorisation des Ressources Naturelles et Assurance
8 Qualité. Faculté SNVST, Université de Bouira, 10000 Bouira, Algeria ;
9 a.imessaoudene@univ-bouira.dz (A.I.) ; l.mouni@univ-bouira.dz (L.M.)

10 ²Laboratoire E2Lim, Université de Limoges, 123 Avenue Albert Thomas, 87060
11 Limoges, France ; jean-claude.bollinger@unilim.fr (J-C.B.)

12 ³Univ.Rennes, ENSCR, 11 Allée de Beaulieu, 35708 Rennes, France ;
13 abdelkrim.bouzaza@ensc-rennes.fr (A.B.) abdeltif.amrane@univ-rennes1.fr (A.A.)

14 ⁴Pharmaceutical Engineering Department, Process Engineering Faculty, Salah
15 Boubnider Constantine 3 University, Constantine, Algeria;
16 hichemm.tahraouii@gmail.com (H.T.)

17
18 * Correspondence: a.hadadi@univ-bouira.dz +213-561-456591.

33

34 **Abstract**

35 Consideration is now being given to the use of metal coagulants to remove
36 turbidity from drinking water and wastewater. Concerns about the long-term impact of
37 non-biodegradable sludge on human health and the potential contamination of aquatic
38 systems are gaining popularity. Recently, alternative biocoagulants have been
39 suggested to address these concerns. In this study, using a 1 M sodium chloride (NaCl)
40 solution, the active coagulating agent was extracted from *Pinus halepensis* Mill. seed,
41 and used for the first time to remove Congo red dye, the influence of numerous factors
42 on dye removal was evaluated in order to make comparisons with conventional
43 coagulants. The application of biocoagulant was shown to be very successful, with
44 coagulant dosages ranging from 3 to 12 mL L⁻¹ achieving up to 80% dye removal and
45 yielding 28 mL L⁻¹ of sludge. It was also found that biocoagulant is extremely pH
46 sensitive with an optimum operating pH of 3. Ferric chloride, on the other hand,
47 achieved similar removal rate with higher sludge production (46 mL L⁻¹) under the same
48 conditions. A Fourier Transform Infrared Spectroscopy and proximate composition
49 analysis were undertaken to determine qualitatively the potential active coagulant
50 ingredient in the seeds and suggested the involvement of proteins in the coagulation-
51 flocculation mechanism. The evaluation criteria of the Support vector machine_Gray
52 wolf optimizer model in terms of statistical coefficients and errors reveals quite
53 interesting results and demonstrates the performance of the model, with statistical
54 coefficients close to 1 ($R = 0.9998$, $R^2 = 0.9995$ and $R^2 \text{ adj} = 0.9995$) and minimal
55 statistical errors (RMSE = 0.5813, MSE = 0.3379, EPM = 0.9808, ESP = 0.9677 and
56 MAE = 0.2382).

57 The study findings demonstrate that *Pinus halepensis* Mill. seed extract might
58 be a novel, environmentally friendly, and easily available coagulant for water and
59 wastewater treatment.

60

61 **Keywords:** *Pinus halepensis* Mill. seed extract; biocoagulant; Congo red; coagulation-
62 flocculation mechanism; Support Vector Machine, Gray Wolf Optimizer.

63

64

65

66

67 **1. Introduction**

68 Synthetic dyes are a significant class of recalcitrant organic compounds that are
69 frequently found in the environment because of their widespread use in several
70 industries; they are considered the most polluting of all industrial sectors. Dye
71 wastewater discharged onto surface waters such as rivers and lakes lowers light
72 transmission in the water, resulting in the reduction of photosynthesis as well as the
73 quantity of dissolved oxygen. Several researches stated that certain colors may
74 degrade and generate carcinogenic aromatic amines that are believed to remain in the
75 environment for a very long period (Momeni et al., 2018). As a result, there is an
76 unavoidable requirement for a dye/color removal method that is both successful and
77 cost-effective under the aforementioned circumstances (Crini et al., 2019; Mouni et al.,
78 2018).

79 Azo dyes are compounds with one or more azo linkages consisting of a
80 diazotized amine linked to an amine or phenol. The principal precursors of azo dyes
81 are aromatic amines. Almost two-thirds of all synthetic dyes are azo compounds.
82 Indeed, they are the most widely used and structurally diverse class of organic dyes
83 on the market owing to the vivid colors they exhibit (Ali et al., 2022). Azo dyes are also
84 stable to light and resistant to microbial degradation or discoloration caused by
85 washing. Therefore, it is difficult to remove these compounds from wastewater using
86 conventional wastewater treatment methods. It is estimated that around 10% of dyes
87 used in textile dyeing procedures do not adhere to fibers and are thus discharged into
88 the environment (Liu et al., 2022). The recalcitrance of azo dyes, attributable to the
89 presence of azo bonds and sulphonate groups (Radhika and Aruna, 2022), and their
90 effects on the environment and human health makes their degradation not only a major
91 environmental concern but also a challenge (Katheresan et al., 2018).

92 Commercially accessible treatment approaches involve either removal or
93 destructive techniques depending on the content of the effluent. Coagulation (Hadadi
94 et al., 2022b; Sun et al., 2021; Tahraoui et al., 2022c), adsorption (Bouchelkia et al.,
95 2022; Imessaoudene et al., 2022), and membrane separations (Dasgupta et al., 2015)
96 are frequent removal procedures, whereas biological treatments (Adenan et al., 2022),
97 advanced oxidation processes (Muniasamy et al., 2020), cavitation (Zampeta et al.,
98 2021), and incineration are destructive approaches. Regardless of the evolution of

99 technologies, there will always be a requirement for the use of coagulation in water
100 and wastewater treatment, since it is regarded one of the simplest and cost-effective
101 methods for enhancing the removal of pollutants from water (Kristianto et al., 2019).

102 Coagulation-flocculation technique refers to a physico-chemical process
103 involving the use of a coagulant that neutralizes the negative charges in the polluted
104 water, thereby reducing the electrostatic repulsion of the electric double layer; this is
105 known as the destabilization process, it begins with an increment in ionic strength,
106 which helps to promote double-layer compression, and/or with neutralization process
107 of the particles surface charge by adsorption of anions (Alnawajha et al., 2022). These
108 destabilized particles aggregate to form more or less large flocs via free precipitation
109 or air flotation; these flocs are finally separated from the contaminated water (Han et
110 al., 2022). Coagulation–flocculation has been used efficiently in several industries
111 because to its simplicity of operation, relatively easy installation, and few energy
112 requirements. Additionally, owing to the process’s adaptability, coagulation–
113 flocculation may be employed as a pre-treatment, a post-treatment, as well as the main
114 treatment of wastewater (Vicente et al., 2022).

115 In reality, the most often employed chemical coagulants are divided into two
116 groups: those consisting of aluminum, such as aluminum sulfate, sodium aluminate
117 and aluminum chloride, and those derived from iron salts, such as ferric sulfate, ferric
118 chloride, ferrous sulfate, or ferric chloride sulfate. Rarely is the usage of these
119 compounds without consequences. Numerous environmental issues relating to the
120 long-term toxicity of coagulants/flocculants are currently being explored, particularly for
121 environmental observers worldwide. In addition to environmental impacts, there are
122 also health concerns related to their use, metallic-based coagulants/flocculants are
123 resistant to biodegradation and degradation, and when absorbed, their residuals in
124 drinking water may have a direct impact on human health and accumulate in body
125 cells. Indicators of the impact of chemical coagulants/flocculants on human health
126 include malfunction of the central nervous system, dementia, Alzheimer's disease, and
127 extreme shaking (Hadadi et al., 2022a). It is also known that they have several
128 disadvantages, including high cost and high sludge production, which lead to additional
129 water treatment (Zhang et al., 2022).

130 Biocoagulants and bioflocculants may be a viable substitute for chemical
131 coagulants and flocculants to minimize environmental pollution and health hazards

132 related with their usage (Šuvalija et al., 2022). Biocoagulants and biofloculants are
133 derived from living organisms or their components and are completely organic and
134 biodegradable; hence, they are ecologically beneficial and have a negligible effect on
135 human health (Adnan et al., 2017). Therefore, to develop these eco-friendly materials,
136 several steps must be followed before they are used in treatment processing units.
137 Many biocoagulants and biofloculants produced from various sources have previously
138 been studied and have shown strong promise as alternatives to chemicals that are
139 currently widely used, including *Moringa oleifera*, a highly promising alternative
140 (Hadadi et al., 2022b; Kapse and Samadder, 2021; Nhut et al., 2021), rice starch (Teh
141 et al., 2014), *Lens culinaris* (Chua et al., 2019), potato starch (Lapointe and Barbeau,
142 2017), *Dillenia indica* (Manholer et al., 2019), *Jatropha curcas* (Abidin et al., 2011),
143 *Nephelium lappaceum* (Zurina et al., 2014), etc. Plant-based coagulants are easy to
144 use, need little processing, and have the potential to provide a sustainable treatment
145 solution. Despite the fact that a number of biocoagulants have been widely explored
146 for practical applications, only a handful have been investigated in detail (Chethana et
147 al., 2016).

148 In this research, we investigate the efficacy of a novel biocoagulant, *Pinus*
149 *halepensis* Mill. seed extract, in treating synthetic water containing Congo red, a well-
150 known carcinogenic and poisonous azo dye. As far as we know, the use of this
151 biomaterial as a coagulant for the removal of dyes has not been previously reported,
152 and biocoagulation investigations have shown very little interest in it (Hadadi et al.,
153 2022a). *Pinus halepensis* Mill., commonly referred to as Aleppo pine, is the most
154 abundant tree in the Mediterranean Basin, particularly in Algeria and Tunisia, and is a
155 member of the 62 Pinaceae family (Ávila et al., 2022). These trees are characterized
156 by their rapid growth, high propagule production, and adaptability to their native areas
157 (Bello-Rodríguez et al., 2020). It has been reported that seeds exhibit a high proteins
158 content (Al-Ismail et al., 2018), making them potential candidates as biocoagulant. The
159 use of an active coagulant in the form of an extract has been favored over the direct
160 use of seed powder; this will decrease the amount of organic matter associated with
161 active coagulant substances, which increases BOD and COD levels in treated water
162 (Baptista et al., 2017).

163 In this work, we investigated the influence of parameters such as coagulant
164 dosage, initial pH, NaCl concentration, slow stirring speed and duration, solution

165 temperature and initial dye concentration on the Congo red removal efficiency.
 166 Moreover, a Support Vector Machine (SVM) coupled with the Gray Wolf Optimizer
 167 (GWO) was used to predict the removal rate of Congo red based on the optimized
 168 parameters of the biocoagulation process. Whereas SVM has lately garnered a
 169 significant deal of interest as an excellent modeling technique for water treatment
 170 systems, GWO technique has been utilized to handle a broad range of optimization
 171 problems, such as enhancing machine learning performance by optimizing model
 172 hyper-parameters. To our knowledge, such work has never been done before.

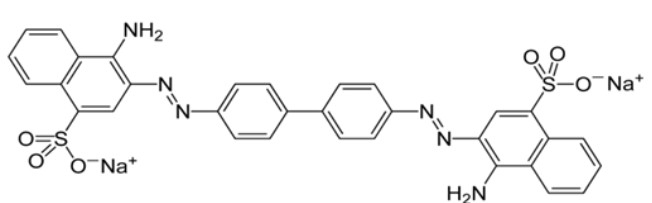
173 2. Material and methods

174 2.1. Chemicals and materials

175 Hydrochloric acid (HCl), sodium hydroxide (NaOH), Hexane, Bradford reagent,
 176 Albumin from bovine serum (BSA), Iron (III) chloride hexahydrate ($\text{FeCl}_3 \cdot 6 \text{H}_2\text{O}$), of
 177 high purity ($\geq 99\%$). and NaCl (all from Sigma Aldrich Chemical Company, USA) were
 178 employed for this investigation; Congo red was purchased from Biochem-
 179 Chemopharma, France.

180 Congo red dye was chosen as the model substance in this research and was
 181 dissolved in distilled water at a concentration of 1 g L^{-1} ; this stock solution was then
 182 diluted to generate solutions with the desired concentrations, and the required pH
 183 value was adjusted by using either 0.1 M HCl or NaOH solutions. Detailed informations
 184 about the structure and characteristics of the dye are presented in **Table 1**.

185 **Table 1** Congo red properties

Dye	Congo red
Chemical class	Di-azo dye
Chemical formula	$\text{C}_{32}\text{H}_{22}\text{N}_6\text{Na}_2\text{O}_6\text{S}_2$
Molar mass (mol/g)	696.665
Maximum wavelength absorbance (λ_{max})	500 nm
Dye content	+ 75 %
Color change at pH	At [pH < 3.0] → Blue color/ At [pH > 5.0] → Red color
Chemical structure	

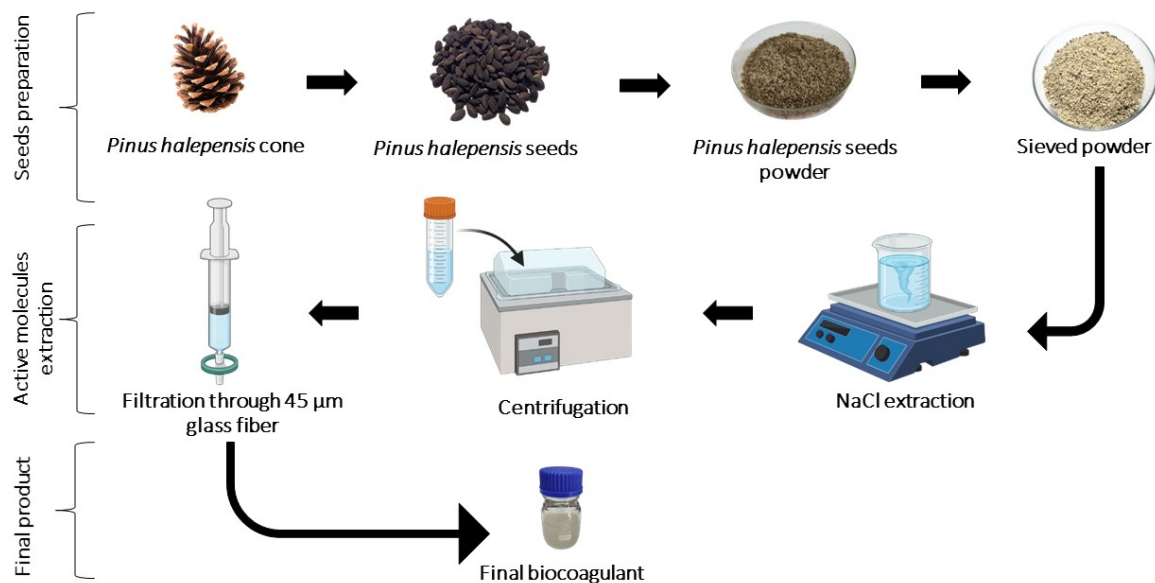
186

187 2.2. *Pinus halepensis* seed preparation and proximate composition analysis

188 *Pinus halepensis* Mill. seeds were purchased from a local herbal market,
189 thoroughly cleaned using distilled water to remove dust and impurities, oven-dried at
190 40°C for 24 hours (Memmert GmbH + Co.KG, Germany), crushed and powdered using
191 a domestic food processor, and sieved through a 500 µm sieve to promote the full
192 solubilization of active components in the coagulant (Hadadi et al., 2022a). To avoid
193 any deterioration of the active ingredients, the obtained powder was stored in sealed
194 amber-glass vial under refrigeration (4°C) until analysis. Moisture and ash contents
195 were determined using the AOAC method: about 3 g of the sample were dried at 105°C
196 during 3 hours before being transferred to a desiccator to cool. The moisture content
197 per 100 g of sample was estimated as the percentage change in weight before and
198 after oven drying. Ash content was determined by incinerating 5 g of the sample in a
199 muffle furnace (Nabertherm GmbH, Lilienthal, Germany) at 550°C for 6 h. The total
200 ash per 100 g of sample was represented as the weight of the greyish-white residue
201 obtained. Crude fat was determined using a Soxhlet apparatus; 20 g of the sample
202 was extracted in hexane under reflux for 8 h, and the extract was quantified as crude
203 fat per 100 g of the sample. Proteins content was expressed using the Bradford method
204 (Kielkopf et al., 2020), total carbohydrates were determined by difference.

205 2.3. Coagulant extraction

206 Salt extraction is recognized as a good approach for isolating proteins that may
207 behave as a polyelectrolyte during the coagulation process. According to previous
208 studies, NaCl was selected as the most suitable salt, owing to its availability and
209 economic advantages (Dalvand et al., 2016; Kristianto et al., 2019). The extraction was
210 performed following the steps shown in **Fig. 1**: 5 g of *Pinus halepensis* Mill. seed
211 powder were stirred with 100 mL of 0.1 to 2 M NaCl solution for 30 minutes; the
212 obtained suspension was centrifuged (Hettich Lab Technology, France) at 1006 xg for
213 10 min and filtered through 45 µm fiberglass. To improve repeatability and avoid aging
214 effects such as pH, viscosity, and coagulation effectiveness changes caused by
215 microbial biodegradation during storage process, a fresh solution of the coagulant was
216 prepared for each sequence of experiments, the resulting extract is referred to as
217 PhsEXT.



218

219

Fig. 1. Biocoagulant preparation steps.

220

221 2.4. Experimental procedure

222 Coagulation experiments were undertaken by using one-factor-at-a-time
 223 (OFAT) method, the trials were performed in 1 L beakers using a jar-test apparatus
 224 (VELP Scientifica Srl, Italy), each beaker was filled with 200 mL of the dye solution at
 225 desired concentrations (50 to 170 mg L⁻¹), pH values (3 to 10), dosages of freshly
 226 prepared PhsEXT (3 to 12 mL L⁻¹) and temperatures (10 to 60°C). The biocoagulant-
 227 dye mixture was rapidly agitated at 200 rpm for 3 min, then the mixing was reduced to
 228 lower speeds (0 to 110 rpm) for 0 to 30 min; flocs were given time to settle (for 0 to 40
 229 min). Following that, samples (20 mL) were collected using a volumetric pipette at 3
 230 cm below the mixture surface (Dalvand et al., 2016) and then centrifuged (1006 xg for
 231 10 min). The final concentrations of the dye were determined using a
 232 spectrophotometer (Agilent Cary 60 UV-Vis, USA). The measurement is performed at
 233 500 nm for the pH range 5–10 and at 562 nm for pH range 3–4. At these wavelengths,
 234 pH-specific calibration curves are developed and used. All studies were repeated three
 235 times. The % removal of Congo red dye R (%) was calculated using Eq. (1):

236

237

$$R(\%) = \frac{C - C_f}{C} \times 100 \quad (1)$$

238 where C (mg L^{-1}) and C_f (mg L^{-1}) represent the initial and residual dye concentrations,
239 respectively.

240 2.5. Morphology of flocs

241 For morphological observations, an optical microscope (Kern & Sohn, Germany)
242 equipped with a mobile camera was used. A drop containing flocs of a fresh dye-
243 PhsEXT mixture was carefully placed on a glass slide and covered with a coverslip. It
244 was immediately observed at x100 magnification to get the pictures.

245 2.6. Support vector machine (SVM)

246 Vapnik developed the support vector machine in the 1990s (Vapnik et al., 1996),
247 it is founded on the statistical learning theory (SLT) techniques and structural risk
248 minimisation (SRM) concept (Wang et al., 2022). Its primary applications were
249 regression analysis and non-linear classification (Bargagli Stoffi et al., 2022). A training
250 data set of N points (X_i, Y_i) is examined in this technique, with $i = 1, N$. X denotes the
251 inputs of the model and Y its output. A SVM model appears like:

$$252 \quad \quad \quad 253 \quad \quad \quad y(x) = \omega^T \phi(x) + b \quad (2)$$

254 where $\phi(\cdot): R^n \rightarrow R^m$ is a non-linear function that maps the finite dimensional space
255 entry into a higher dimensional space that is implicitly created, ω represents a weight
256 vector, and b is the bias (Suykens et al., 2002; Vapnik et al., 1996).

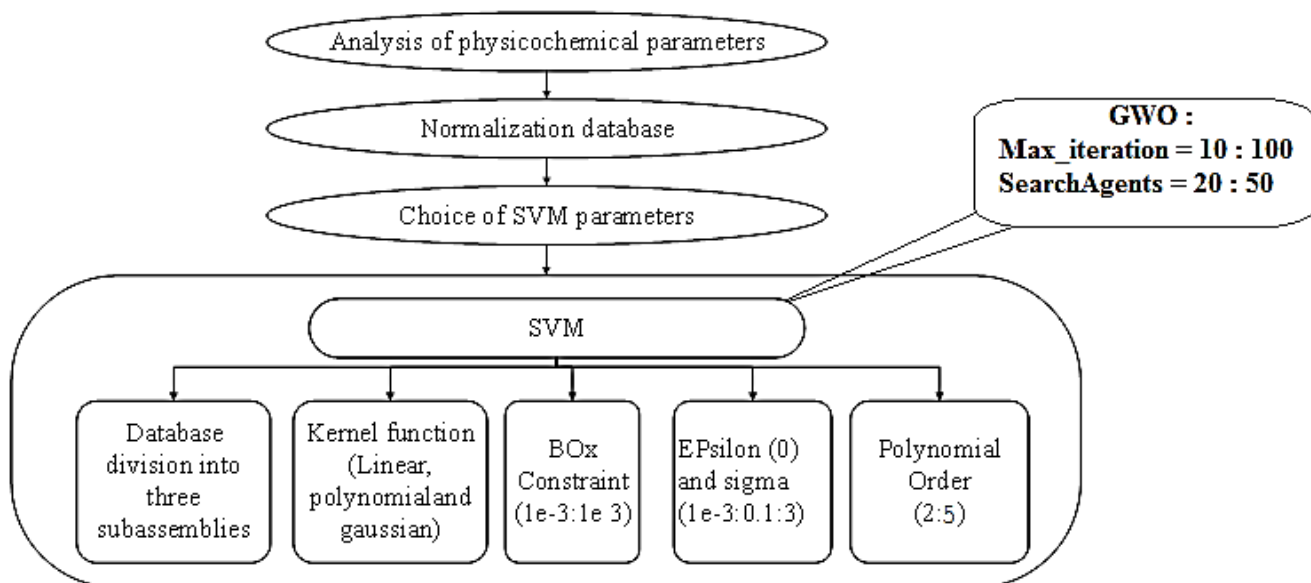
257
258 In this study, the SVM model was chosen for the prediction of the removal rate of
259 Congo red by the PhsEXT using the Matlab R2020a software. For this purpose, the
260 results of the parameter optimization (part "2.4. Experimental procedure") for the
261 removal of Congo red were compiled into a single database, which has 8 input
262 parameters and one parameter Release

263 The independent parameters were the slow stirring time (X1), the sedimentation
264 time (X2), the initial concentration of Congo red (X3), the dose of biocoagulant (X4),
265 the pH of the solution (X5), the concentration of NaCl (X6), The slow stirring speed
266 (X7) and temperature (X8). In contrast, the dependent parameter was the removal rate
267 of Congo red (Y).

268 To obtain the optimal result from SVM, the Gray Wolf Optimizer (GWO) algorithm was
269 coupled with SVM (SVM_GWO) in order to optimize the parameters of each kernel

270 function. As a result of its remarkable capacity to enhance model performance via
 271 hyper-parameter optimization (Colombo, 2017; Mirjalili et al., 2014).

272 To construct the model, the MATLAB software Help guide was used, this design is
 273 shown in the following illustration:



274

275 **Fig. 2.** Organization chart for SVM mode development and optimization.
 276

277 Where:

278 • The database was normalized once in the interval [-1, +1] using MATLAB's
 279 "mapminmax" function. Next, the database was split into two: 80% of the dataset
 280 for training and 20% of the validation samples.

281 • The kernel functions that have been selected in this study are as follows:
 282 (Benimam et al., 2020).

283 • Poly (polynomial)

$$284 \quad k(X_i, X_j) = (ax^T + c)^d \quad (3)$$

285

286 • Linear

$$287 \quad k(X_i, X_j) = x^T y + c \quad (4)$$

288 • Gaussian

$$289 \quad k(X_i, X_j) = \frac{1}{\sigma\sqrt{2\pi}} \exp\left\{\frac{-X_i - X_j^2}{2\sigma^2}\right\} \quad (5)$$

290

291 with $C = \text{BOxConstraint}$, $d = \text{Polynomial Order}$, $\varepsilon = \text{epsilon}$ and $\sigma^2 = \text{sigma}$ where d , c ,
 292 ε , and σ^2 are the defined kernel parameters.

293

294 2.7. Statistical criteria

295

296

297

298

299

300

301

302

Statistical criteria were used to evaluate the performance and select the best model, including the Correlation Coefficient (R), the Coefficient of Determination (R^2), the Adjusted Coefficient (R^2_{adj}), the Mean Square Error (MSE), the Root Mean Square Error (RMSE), and the Mean Absolute Error (MAE). Error Standard of Prediction (ESP) and Error Prediction of Model (EPM) were also considered. These criteria are calculated considering the following equations (Bousselma et al., 2021 ; Tahraoui et al., 2020, 2021a, 2021b, 2022a, 2022b).

303

$$R^2_{adj} = 1 - \frac{(1-R^2)(N-1)}{N-K-1} \quad (6)$$

304

$$RMSE = \sqrt{\left(\frac{1}{N}\right) \left(\sum_{i=1}^N [(y_{exp} - y_{pred})]^2\right)} \quad (7)$$

305

$$MSE = \left(\frac{1}{N}\right) \left(\sum_{i=1}^N (y_{exp} - y_{pred})^2\right) \quad (8)$$

306

$$MAE = \left(\frac{1}{N}\right) \sum_{i=1}^N |y_{exp} - y_{pred}| \quad (9)$$

307

$$ESP(\%) = \frac{RMSE}{\bar{y}_{exp}} \times 100 \quad (10)$$

308

$$EPM(\%) = \frac{100}{N} \sum_{i=1}^N \left| \frac{(y_{exp} - y_{pred})}{y_{exp}} \right| \quad (11)$$

309

310

311

312

Where N is the number of data samples; K is the number of variables (inputs); \bar{y}_{exp} and y_{pred} are the experimental and the predicted values respectively; \bar{y}_{exp} and \bar{y}_{pred} are the average values of the experimental and the predicted values, respectively (Bousselma et al., 2021; Tahraoui et al., 2021a, 2021b, 2022a, 2022b).

313 3. Results and discussion

314 3.1. Physicochemical characterization

315 The physicochemical characteristics of *Pinus halepensis* Mill. seeds are presented in
316 **Table 2.**

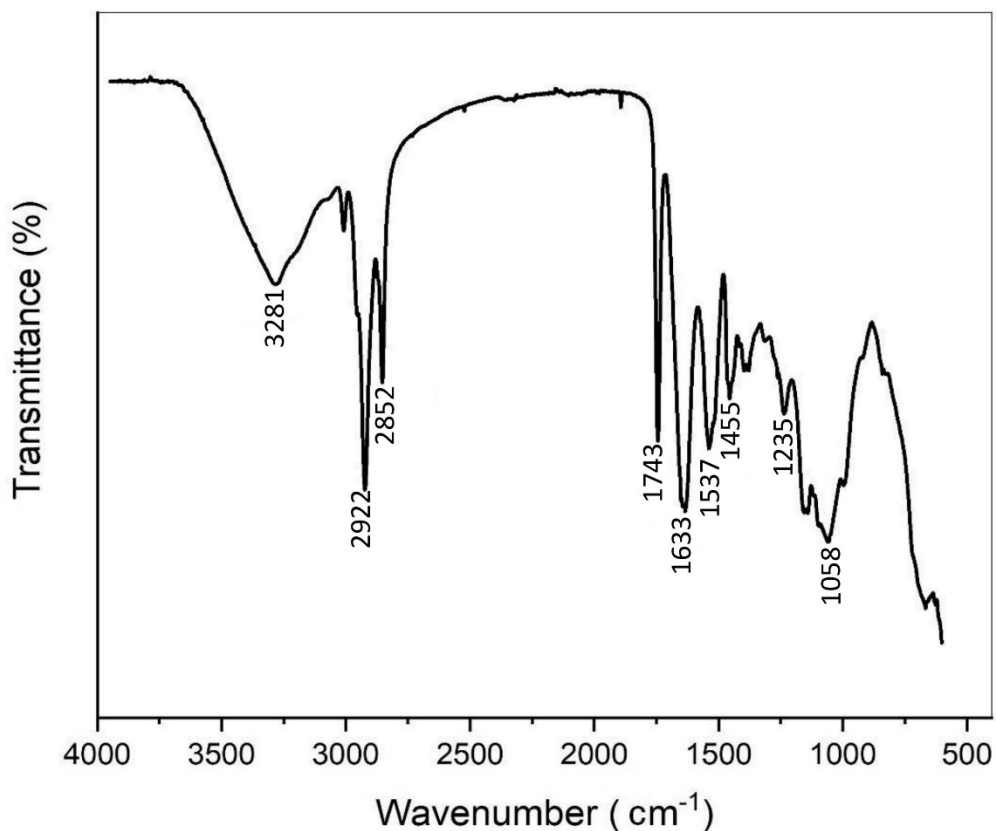
317 The moisture level was 2.3 g/100g, while the ash content was 4.6 g/100g. The
318 seeds had a considerable amount of fat: 31.10 g/100 g. Although pine seeds are
319 typically rich in oils, their composition varies based on species and environmental
320 factors (Dziedziński et al., 2021). Total carbohydrates were 31.4 g/100 g (per
321 difference). The proximate proteins content reached 30.6 g/100 g. Tukan et al. (2013)
322 observed that the proteins level of raw or cooked *Pinus halepensis* Mill. seeds could
323 reach more than 29%; these data suggest a high concentration of proteins capable of
324 acting as a coagulant agent in our investigation.

325 **Table 2** Chemical composition of Aleppo Pine (*Pinus halepensis* Mill.) seeds. (mean±
326 SD, n= 3)

Composition	Percentage
Dry matter	97.7±0.6
Ash content	4.6±0.1
Crude proteins	30.6±1.2
Fat	31.1±1.2
Total carbohydrates (by difference)	31.4±1.2

327
328 **Fig. 3** shows that numerous main peaks with several intensities were detected
329 at different frequencies in the FTIR spectrum. The broad peak at 3281 cm⁻¹ can be
330 ascribed to the stretching vibrations of the –OH groups indicating the presence of the
331 functional groups alcohol, phenol, carboxylic group and –NH stretching of amide and
332 amines groups (Ghodke et al., 2021), which appear predominantly in the
333 carbohydrates, polysaccharides (Saldarriaga-Hernández et al., 2021), proteins and
334 fatty acid structures present in the *Pinus halepensis* Mill. seeds. The sharp peak in the
335 vicinity of 2922 cm⁻¹ was related to the C-H stretching of either alkane (Ghodke et al.,
336 2021) or carboxylic acid (El-Din et al., 2017). 2852 cm⁻¹ was related to the –CH– and
337 CH₂ stretching vibrations found in fatty acids. In the region between 1743 cm⁻¹ and

338 1633 cm^{-1} , there are strong peaks linked to C=O bond stretching, carbonyl group is
339 present in proteins and fatty acids. The peak at 1537 cm^{-1} is attributed to the bending
340 of NH_2 (amine) group (Putra et al., 2020); the presence of this band demonstrates that
341 *Pinus halepensis* Mill. seeds have a protein structure containing amino groups. Bands
342 at 1455 cm^{-1} and 1235 cm^{-1} correspond to the C-O stretching of carboxylic acids and
343 phenolic compounds, while that at 1058 cm^{-1} correspond to the C-O stretching of
344 polysaccharides (Araújo et al., 2016). Similar FTIR spectra have been observed in
345 previous studies on natural coagulants (Amran et al., 2021; Hussain and Haydar,
346 2019).
347



348
349
350
351
352

Fig. 3. FTIR spectra of *Pinus halepensis* Mill. seeds.

353 3.2. Factors affecting the coagulation process

354 3.2.1. Effect of initial pH on Congo red removal

355 pH is a crucial parameter in the coagulation–flocculation process since it
356 influences the biocoagulant surface charge and the stabilization of the dye wastewater.
357 **Fig. 4(a)** depicts the influence of pH throughout a pH range of 3 to 10 (Due to Congo
358 red precipitation, lower pH values were neglected); very acidic conditions promote
359 effective Congo red removal, with a maximum percentage of 80.46% at pH = 3. The
360 removal rate decreases dramatically as pH continues to rise. This result is consistent
361 with previous studies (Chethana et al., 2016; Tie et al., 2015b); Since proteins are
362 believed to be the active agent in coagulation, their amino groups may get protonated
363 under acidic conditions, enhancing their interaction with the anionic portion of the dye
364 (sulfite SO_3^{2-} groups). A further rise in pH is expected to cause proteins carboxyl
365 groups to become negatively charged (COO^-), hence increasing the solubility of Congo
366 red due to electrostatic repulsion. The proteinaceous profile of *Pinus halepensis* seeds
367 supported by FTIR and proximate composition analysis results corroborate these
368 assumptions. (Abidin et al., 2011; Bahrodin et al., 2021) reported that the coagulation
369 mechanism is charge neutralization when the difference between maximum removal
370 and minimum removal by using different pH is around 50% or more, which is the case
371 in our investigation. Also, bridging cannot be considered as a possible mechanism
372 because unlike charge neutralization, bridging is least affected by pH. however, at
373 lower pH, the polymeric chains responsible for interparticle bridging will expand and
374 be able to attach to additional pollutants (Momeni et al., 2018; Zaidi et al., 2022). Using
375 aluminum sulfate, Vijayaraghavan et al. (2015) observed a 74% Congo red removal
376 rate under the same acidic conditions and initial dye concentration of 50 mg L^{-1} , while
377 Kristianto et al. (2021) reported that ferric chloride removed 30% of the dye (Congo
378 red initial concentration = 50 mg L^{-1} , pH = 6.5).

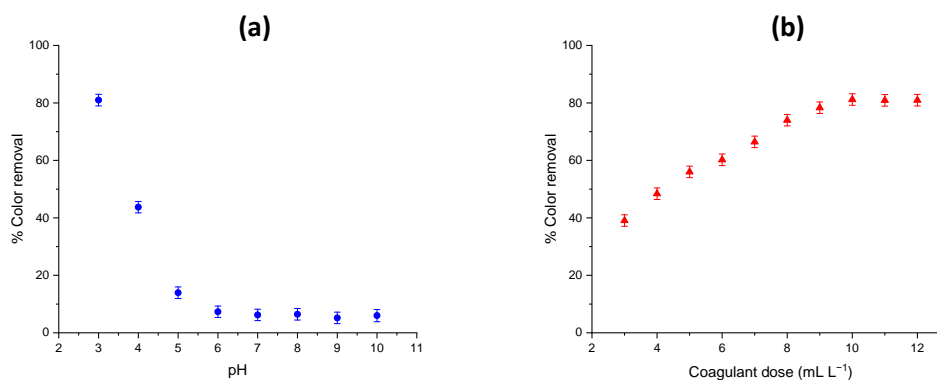
379 3.2.2. Effect of coagulant dosage on Congo red removal

380 Coagulant dosage is a primordial parameter since it determines the cost of the
381 coagulation–flocculation process (Tie et al., 2015a). The experiment was carried out
382 to identify the optimal dose of PhsEXT in terms of Congo red elimination. 50 mg L^{-1} of
383 Congo red were treated with an increasing dose of coagulant (3 to 12 mL L^{-1}). We
384 opted to represent the coagulant dosage in units of mL L^{-1} rather than mg L^{-1} since the

385 filtering step retains around 70% of the insoluble *Pinus halepensis* Mill. seed powder
386 during PhsEXT preparation (Nhut et al., 2021).

387 From **Fig. 4(b)**, it is observed that the increase in the biocoagulant dose
388 increases the percentage removal of Congo red until reaching a plateau, after which
389 additional increases in dosage did not improve the percentage removal; However,
390 Congo red removal decreased when the dosage was further increased up to 12 mL/L
391 (results not shown), this is explained by the fact that the main concept of coagulation
392 is the destabilization of colloidal matter and suspended particles by the introduction of
393 positive species. However, when the coagulant dosage increases, there will be an
394 excess of positive ions, leading the particles to repel one another and the solution to
395 re-stabilize. A dose of 10 mL L⁻¹ gives an optimal dye removal rate of 81.17 %. The
396 interaction between the positive charges of the amino groups and the negative charges
397 of the anionic dye, as previously stated, is thought to explain the coagulation process
398 observed in this work, more dye molecules are destabilized by electrostatic attraction
399 when the coagulant dose is increased, resulting in greater charge neutralization and,
400 thus, a higher dye elimination % (Chethana et al., 2016; Dalvand et al., 2016; Hadadi
401 et al., 2022a; Pardede et al., 2018). Shamsnejati et al. (2015) reported the use of
402 *Ocimum basilicum* as a biocoagulant to eliminate Congo red, achieving a maximum
403 color removal of 68.5% using 1.6 mg L⁻¹ (initial Congo red concentration = 50 mg L⁻¹).
404 Under acidic conditions (pH = 3), a solution of 2 % potato starch was found to remove
405 about 50% of Congo red (Pardede et al., 2018). Mishra et al. (2004) observed that
406 adding 10 mg L⁻¹ of *Plantago psyllium* mucilage to an initial dye concentration of 1 mg
407 L⁻¹ led to the maximum elimination of golden yellow and reactive black, with 71 % and
408 35 %, respectively. *Moringa oleifera* and *Phaseolus vulgaris* extracts at 30 mg L⁻¹
409 removed 83 % and 73 % of Congo red, respectively, with an initial dye concentration
410 of 50 mg L⁻¹ and pH = 4. (Vijayaraghavan and Shanthakumar, 2015). In comparison to
411 previous studies, PhsEXT exhibits a high efficiency in the removal of Congo red dye.

412



413

414 **Fig. 4.** Parameters affecting the removal of Congo red dye by the biocoagulant, (a)
 415 Effect of initial pH of Congo red solutions, (b) Effect of biocoagulant dosage.

416

417 3.2.3. Effect of initial Congo red concentration

418 To examine the effect of the initial dye concentration on the coagulation efficiency,
 419 optimal conditions found earlier (pH = 3, coagulant dose = 10 mL L⁻¹) were applied to
 420 different concentrations of Congo red (50 to 170 mg L⁻¹). **Fig. 5(a)** clearly shows that
 421 increasing the initial Congo red concentration resulted in a decrease in the percentage
 422 of dye elimination from 80.78 % to 43.61 %.; this trend was noticed in earlier studies
 423 (Beltrán et al., 2009; Chethana et al., 2016). As the dye concentration increases, the
 424 coagulant dose becomes insufficient for neutralizing the negative charges in Congo
 425 red dye, and PhEXT becomes exhausted (Beltrán et al., 2009). In conclusion, treating
 426 dye wastewater with a higher initial concentration may need a larger dosage of natural
 427 coagulant by providing more adsorption sites.

428 3.2.4. Effect of NaCl concentration

429 Several NaCl solutions with concentrations of 0.1; 0.5; 1; 1.5; and 2 M were selected
 430 to examine the effect of salt solution concentration on coagulation efficiency. The
 431 results (**Fig. 5(b)**) shows that the coagulation effectiveness of the biocoagulant
 432 increases with an increase in salt concentration. Maximum dye removal (81.51%) was
 433 achieved at 1 M of NaCl. This phenomenon is thought to be caused by the salting-in
 434 mechanism, which refers to the process of increasing the ionic strength of a solution,
 435 hence boosting the solubility of the proteins present in *Pinus halepensis* Mill. seeds,
 436 which are believed to act as a coagulant agent (Dalvand et al., 2016; Madrona et al.,
 437 2010). A further increase in NaCl concentration is expected to result in the opposite
 438 phenomenon, salting out; at high salt concentrations, the solubility of proteins reduces

439 dramatically, resulting in poorer extraction and a low Congo red dye removal %
440 (Megersa et al., 2019; Hadadi et al., 2022b). According to Dalvand et al. (2016) , when
441 the concentration of NaCl rises, chloride ions may compete with dye molecules for
442 attraction with the positive charges on the coagulant surface, resulting in decreased
443 dye removal.

444 *3.2.5. Effect of slow stirring speed on dye removal efficiency*

445 Rapid mixing is often used to promote better chemical dispersion in the
446 suspension, slow stirring is then applied to allow particles to aggregate in larger
447 settleable flocs, According to **Fig. 5(c)**, At a slow agitation speed of 30 rpm, the highest
448 dye removal percentage of 81.80 % was achieved; Increased stirring speed resulted
449 in a decrease in dye removal; this might be attributable to the breakage of existing flocs
450 because of disruptive forces (Teh et al., 2014).

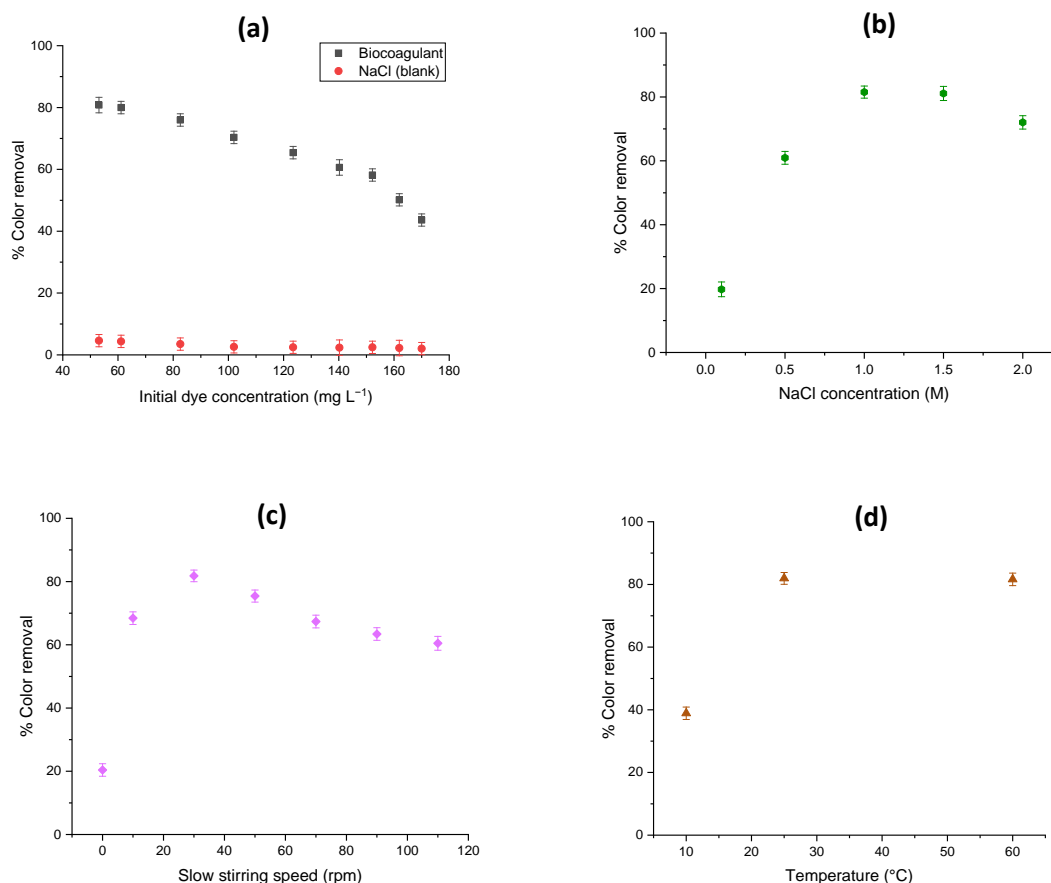
451 *3.2.6. Effect of slow stirring time and floc settling time on dye removal*

452 The settling of generated flocs is the last phase in the coagulation-flocculation
453 process. A faster floc settling rate is advantageous during the coagulation process and
454 shows the efficiency of the coagulant (Daverey et al., 2019). The effect of flocculation
455 mixing time and settling time on Congo red elimination percentages were studied ; time
456 intervals ranging from 0 to 30 minutes were used (data not shown). flocs rapidly settled
457 within the first 5 min, with little fluctuation after 10 min. This phenomenon might be
458 explained by the rapid formation of aggregates of appropriate size that settle rapidly
459 and easily.

460 *3.2.7. Effect of solution temperature on the dye removal efficiency*

461 Although temperature has not been extensively investigated in earlier studies,
462 especially when the coagulation-flocculation process is carried out at temperatures
463 higher than 25°C (Domínguez et al., 2005), given that some textile dyeing effluents are
464 produced at relatively high temperatures, this parameter must be considered.
465 Maintaining earlier parameters at their optimum (pH= 3, coagulant dosage= 10 mL/L,
466 Initial Congo red concentration = 50 mg/L, NaCl concentration = 1 M, Slow stirring
467 speed = 30 rpm, slow stirring time = 20 min, floc settling time = 30 min), temperature
468 was varied from 10 to 60°C, **Fig. 5(d)** depicts the results. It is noteworthy that the dye
469 removal percentage improves from 38.89% to 81.93% when the temperature is

470 increased from 10°C to 60°C; this may be explained by the effect of temperature on
 471 solution viscosity, which rises as temperature decreases, high viscosity has a negative
 472 influence on flocs' collision rates, while low temperature is thought to weaken particle
 473 aggregation in solution, resulting in poor Congo red removal. (Pritchard et al., 2010;
 474 Rodrigues et al., 2013; Tie et al., 2015a).



475

476

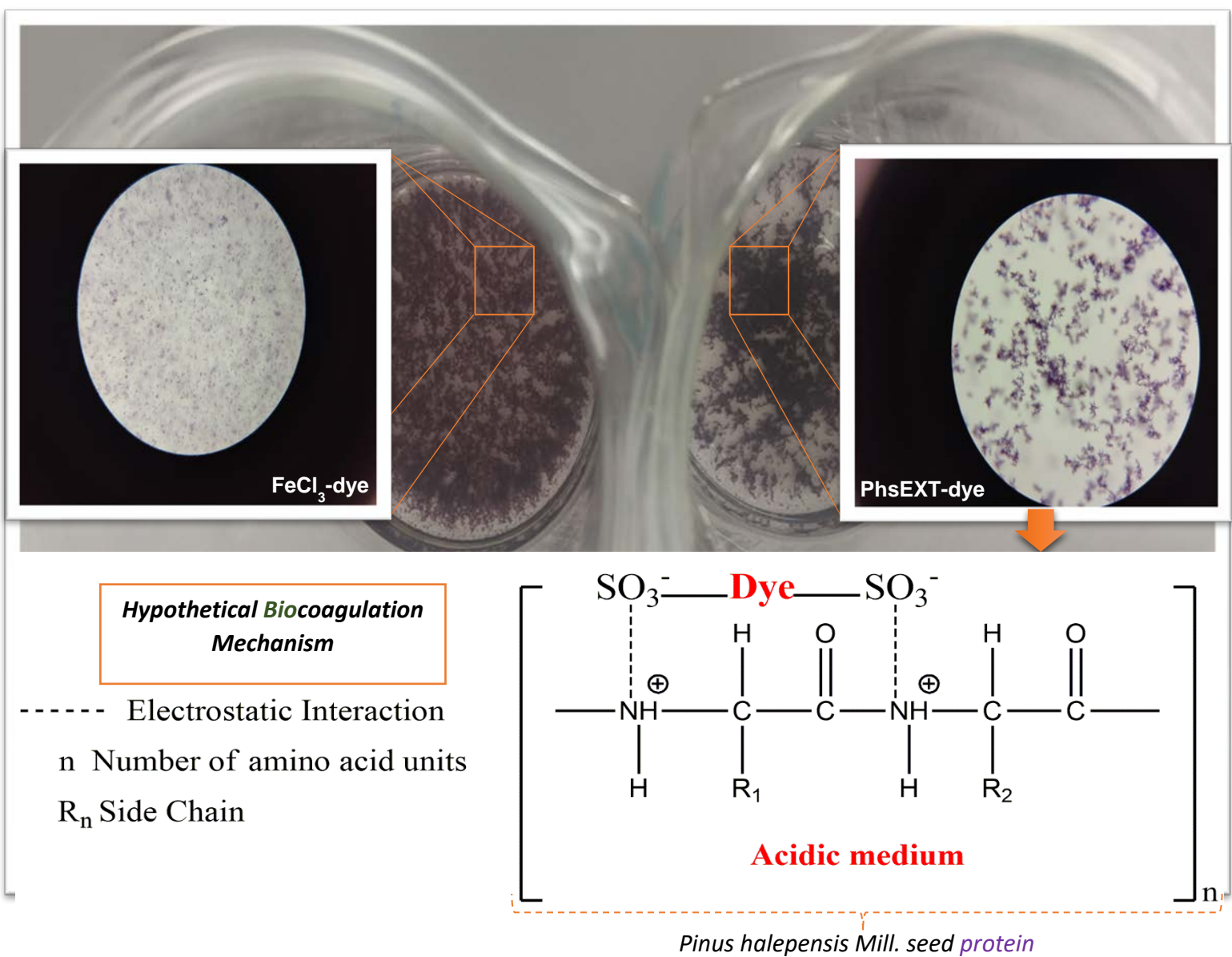
477 **Fig. 5** (a) Effect of Congo red and NaCl (blank) concentrations, (b) Effect of
 478 extraction solution's concentration (NaCl), (c) Effect of slow stirring speed
 479 (flocculation step), (d) effect of Congo red solutions temperature. (Optimal conditions
 480 of each parameter were kept for the next step).

481

482 3.3. Morphology of flocs

483 The size and structure of flocs are considered to be critical to the efficient
 484 functioning of industrial units. The goal of water and wastewater treatment is to remove
 485 contaminants in the form of solid particles from polluted water. After the solid particles
 486 are formed, they may be separated from the treated water using sedimentation,
 487 flotation, filtration, and thickening methods. Consequently, the physical properties of

488 flocs are important in determining their removal efficacy. Using a light microscope, the
 489 formation of flocs was observed in this study for both FeCl₃-dye and PhsEXT-dye (**Fig.**
 490 **6**) (Szygula et al., 2009). Notably, the biocoagulant generated flocs that were thicker
 491 and denser than FeCl₃, which produced flocs that were light, dispersed, and more
 492 fragile. These results suggest that flocs generated with a biocoagulant settle faster
 493 (Pan et al., 1999); This parameter indirectly measures the efficacy of the coagulation–
 494 flocculation process (Aziz and Ramli, 2017) and is a good indication of the suitability
 495 of *Pinus halepensis* Mill. seed-based biocoagulant as an alternative to chemical
 496 coagulants such as FeCl₃.



510
511
512
513
514
515
516
517
518
519
520
521
522
523
524
525
526
527
528
529
530
531
532
533
534
535
536
537
538
539
540

Fig. 6. Microscope observation of floc formation at 100× magnification (pH= 3, dosage 10 mL L⁻¹, C = 50 mg L⁻¹, sampling at 60 min) with hypothetical biocoagulation mechanism occurring in this study.

3.4. Congo red removal Rate modelling using a Support Vector Machine coupled with Gray Wolf Optimizer

In this part, 3 kernel functions were optimized, and each kernel synthesized by the variables must also be optimized: The linear function generated by BOxConstraint, epsilon, and sigma; the Gaussian function synthesized by BOxConstraint, epsilon, and sigma; and the polynomial function generated by BOxConstraint, epsilon, and PolynomialOrder, knowing that PolynomialOrder was optimized from 2 to 5. Using the GWO technique, the variables of each kernel function were optimized.

After acquiring the outcome of the learning phase, the result was confirmed using the validation database. In order to calculate R, R², R²adj, RMSE, MSE, EPM, ESP, and MAE, the generated results (predicted values) were compared with the experimental values in the two phases (the learning phase and the validation phase). The outcomes of these tests are shown in **Table 3**. Note that the findings were denormalized to their actual values in order to be compared to other models.

Table 3 Performances of the different tested SVM Kernel function.

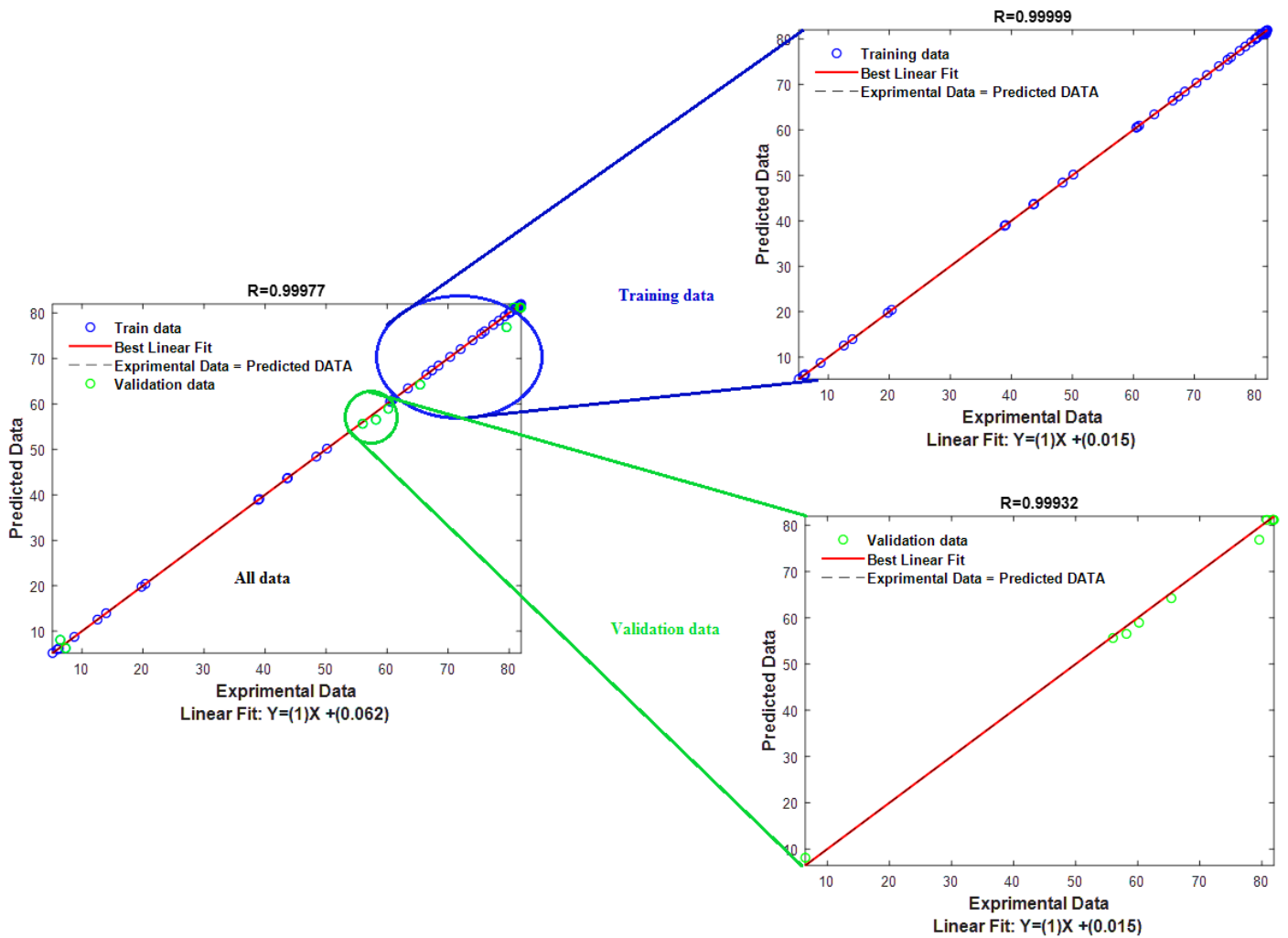
GWO											
Max_iteration=100											
SearchAgents_no=30											
Kernel function	C	ϵ	σ^2	d		R/R ² /R ² _{adj}			RMSE/MSE/EPM/ESP/MAE		
						Train	Val	All	Train	Val	All
Linear	540	208.1278	1.2000	/	45	0.7836	0.5543	0.7573	17.6421	14.4266	17.0584
						0.6140	0.3073	0.5735	311.2425	208.1278	290.9878
						0.5283	0.3073	0.5009	67.9624	15.6305	57.6829
									30.4879	20.8748	28.3954
								11.8560	11.1706	11.7213	
Gaussian	1180	1.6758	1.2000	/	45	1.0000	0.9993	0.9998	0.1045	1.2945	0.5813
						1.0000	0.9986	0.9995	0.0109	1.6758	0.3379
						1.0000	0.9932	0.9995	0.0315	4.8643	0.9808
									0.1738	2.1594	0.9677
								0.0252	1.1094	0.2382	
Polynomial	10	23.1264	/	4.8000	45	0.9945	0.8969	0.9917	2.8729	4.8090	3.3429
						0.9890	0.8044	0.9835	8.2534	23.1264	11.1748
						0.9865	0.0218	0.9807	7.4935	3.9188	6.7913
									5.1037	6.3647	5.5646
								1.7791	3.0117	2.0212	

542

543 By comparing the coefficients and the statistical errors, it is obvious that the
 544 Gaussian function gave the best result; this result is schematized graphically by **Fig.**

545 **7:**

546



548 **Fig. 7.** The relationship between the measured dosage of coagulant and the SVM-
 549 estimated dose.

550 *3.4.1. Model performance test*

551 Interpolation was used to assess the performance of the generated SVM_GWO
 552 model. This was performed by using a cached database comprising 20 experimental
 553 data points that were not used during model training. **Table 4** summarizes the results
 554 in terms of coefficients and statistical errors.

555
 556
 557
 558

559

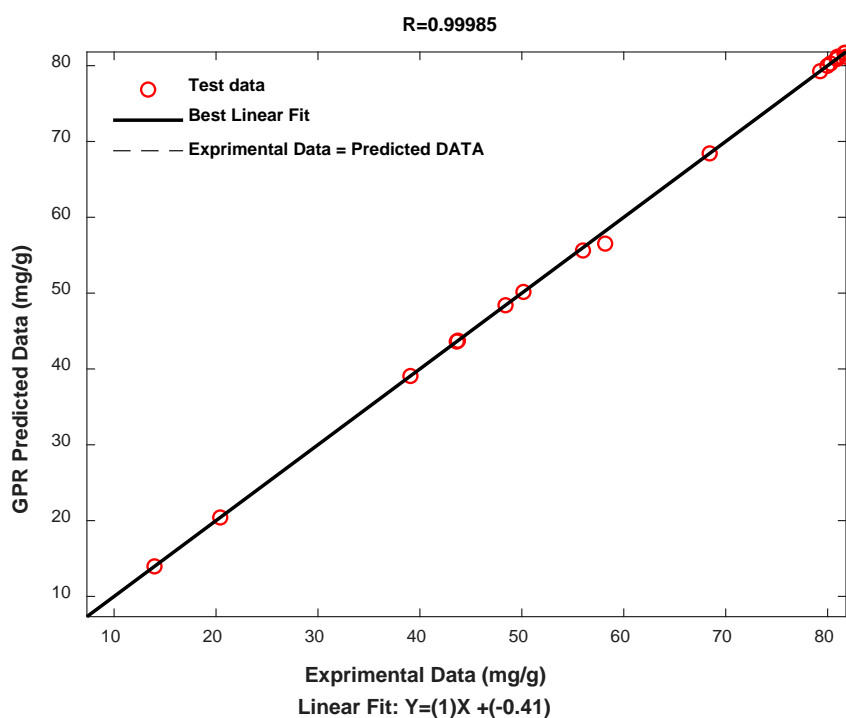
Table 4 Model test performance.

R/R ² / R ² _{adj}	RMSE/MSE/ EPM/ESP/MAE
ALL	ALL
0.9998	0.4675
0.9996	0.2186
0.9994	0.9364
	0.7945
	0.1951

560

561 The coefficients shown in **Table 4** demonstrate the effectiveness and
562 performance of our model.

563 This result was represented graphically (**Fig. 8**) in terms of the experimental
564 values and the predicted values.



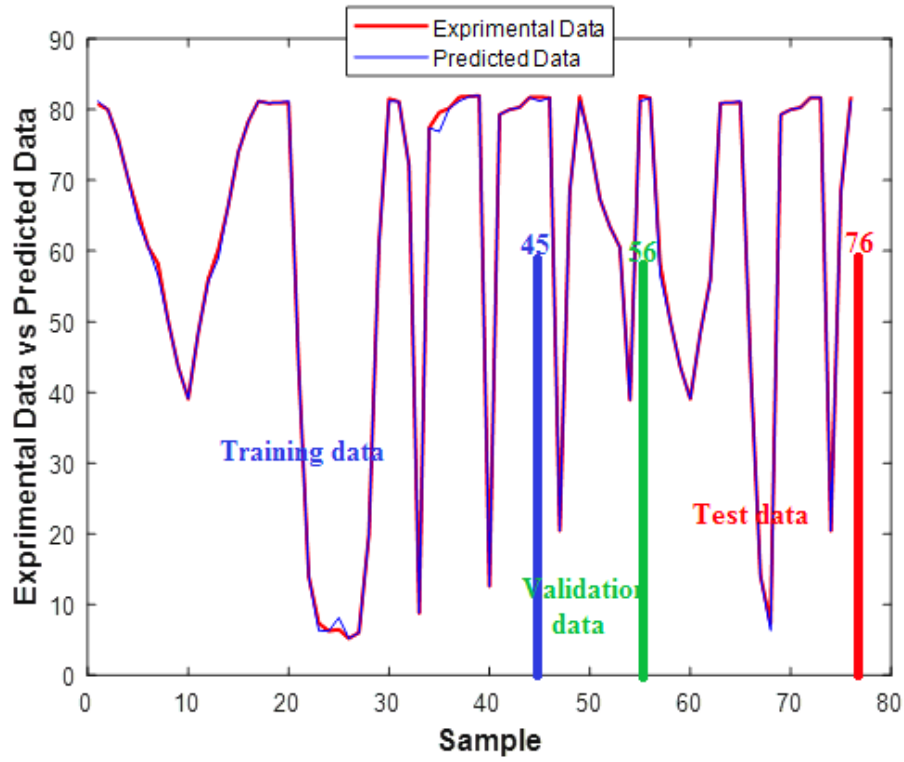
565

566 **Fig. 8.** Comparison between experimental and predicted values to assess
567 performance.

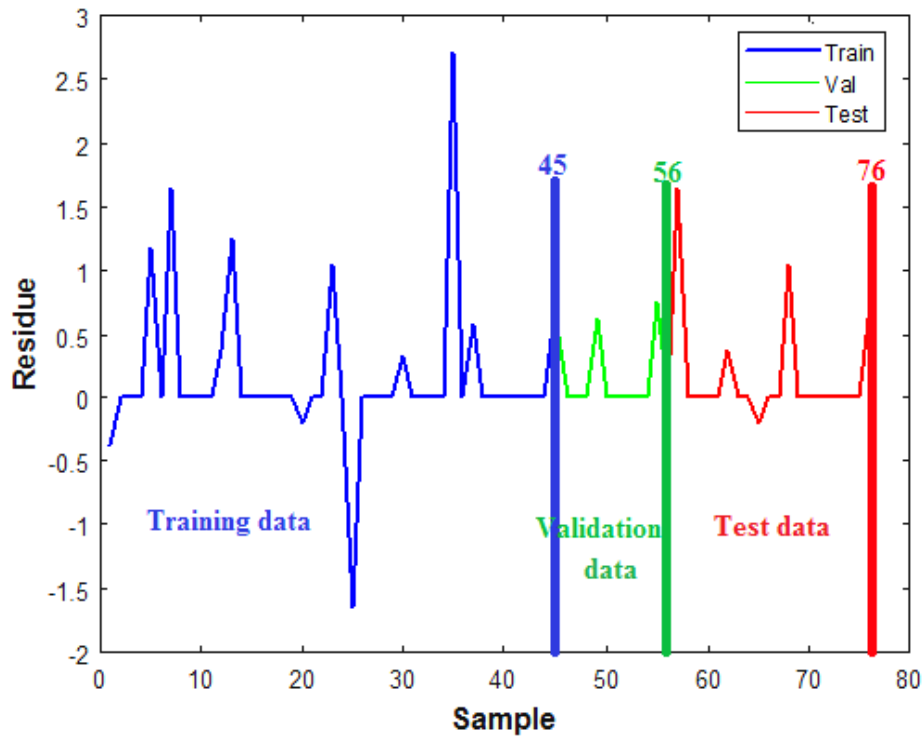
568 3.4.2. *Residues study*

569 The residuals approach was used in this study to investigate the relationship
570 between the experimental and predicted values on the one hand, and the efficiency
571 and performance of the chosen model on the other (Tahraoui et al., 2021b, 2022b).
572 For this purpose, the experimental and predicted values were plotted in parallel as a
573 function of samples (**Fig. 9(a)**) for all data (including data training, data validation and
574 data test performance) (Bousselma et al., 2021; Tahraoui et al., 2022a).

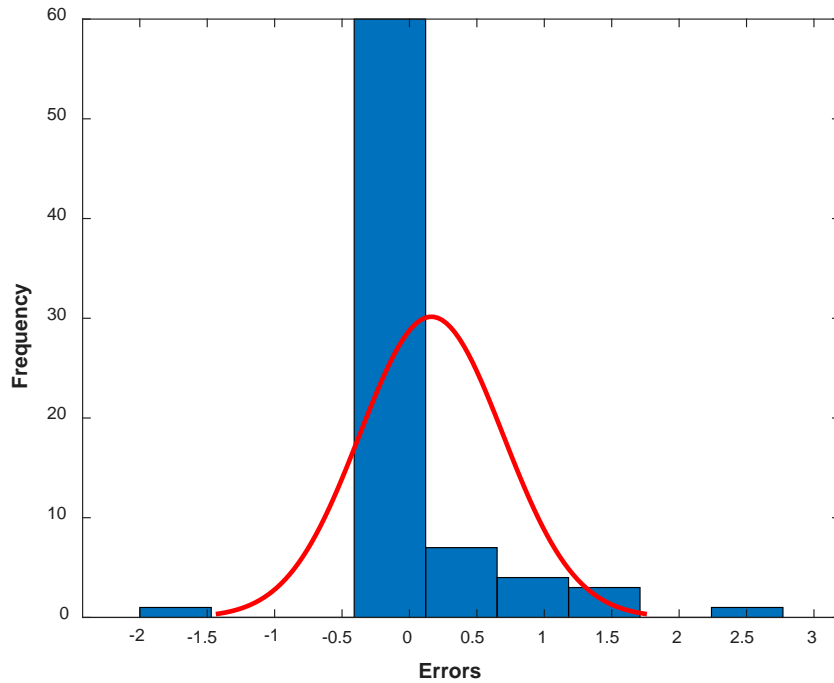
575 In contrast, for all data, the error was determined as the difference between the
576 experimental and predicted values (including data training, data validation and data
577 test performance). This error was plotted graphically (**Fig. 9(b), (c) and (d)**) by three
578 methods (residue, frequency and instances) (Tahraoui et al., 2021a, 2021b, 2022b).



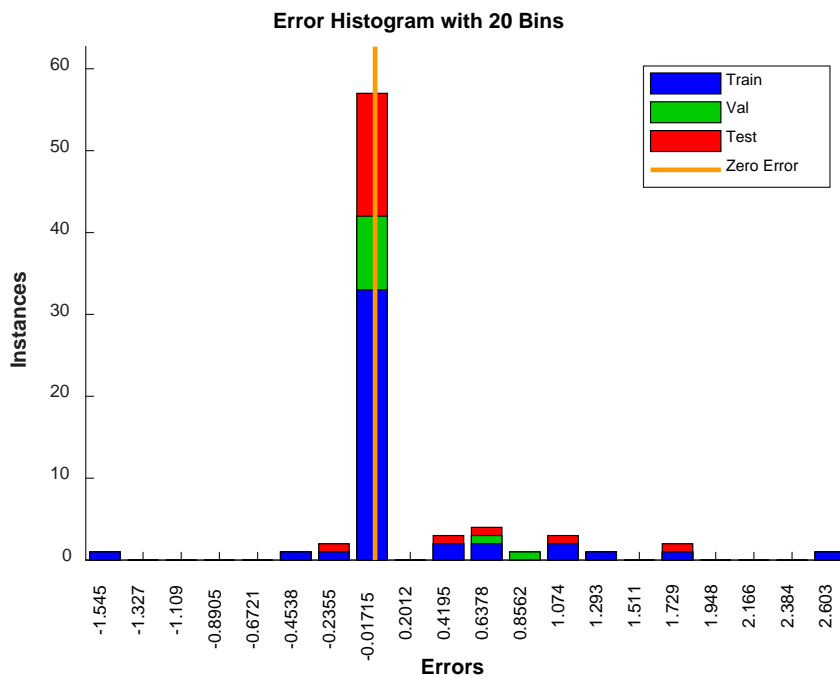
(a)



(b)



(c)



(d)

Fig. 9. Residuals relating to the models established by the different techniques according to the estimated values: (a) Relationship between experimental and anticipated sample data, (b) Residues relating to the models established, (c) Frequency distribution of errors, and (d) Instances distribution of errors.

Fig. 9(a) shows the strong convergence between the experimental values and the predicted values, confirming once again the efficiency of the obtained model.

579 Moreover, **Fig. 9(b)** shows the small errors obtained in the three phases. Indeed,
580 in the learning phase the error did not exceed 3%, the error values were 1% in the
581 validation phase, and 2% for the test phase. It can therefore be concluded that the
582 errors obtained from our model are very small. This was confirmed by examining **Fig.**
583 **9(c) and (d)**, where **Fig. 9(c)** shows that the high frequency was obtained at error 0.
584 Similarly for **Fig. 9(d)**, where most errors were around zero for all three phases
585 (training, validation, and testing data). All these demonstrations and interpretations
586 strongly demonstrate the efficiency and performance of our model.

587

588 3.5. Optimization of the optimal analysis and Validation

589 An optimization method was carried out using GWO to find the optimal conditions
590 for the elimination of Congo red by the biocoagulant.

591 The optimization results revealed ideal conditions for small concentrations, namely
592 up to 150 mg/L ($X_1 = 20$ min, $X_2 = 30$ min, $X_3 = 50$ and 150 mg L⁻¹, $X_4 = 10$ mL L⁻¹,
593 $X_5 = 3$, $X_6 = 1$, $X_7 = 30$ rpm, and $X_8 = 25^\circ\text{C}$). For concentrations greater than 150 mg
594 L⁻¹, the same preliminary conditions as those obtained for the concentration less than
595 150 mg L⁻¹ apply, the only difference is that the temperature must be increased to 60°C
596 ($X_8 = 60$ °C) for an elimination rate of 53.23 % to be achieved. These findings were
597 validated in the laboratory by applying the ideal conditions at various doses (50, 150,
598 and 170 mg L⁻¹). The optimization results are shown in **Table 5** with an error rate of
599 less than 2%, demonstrating our model's effectiveness once again.

600

601

602

603

604 **Table 5** Results of the removal rate of Congo red under the optimal conditions.

GWO: X1 = 20 min, X2 = 30 min, X3 = 50 mg L ⁻¹ , X4 = 10 ml L ⁻¹ , X5 = 3, X6 = 1 M, X7 = 30 rpm and X8 = 25°C	
The predicted removal rate of Congo red (%)	81.17
The experimental removal rate of Congo red	81.93
Error (%)	0.79
GWO: X1 = 20 min, X2 = 30 min, X3 = 150 mg L ⁻¹ , X4 = 10 mL L ⁻¹ , X5 = 3, X6 = 1 M, X7= 30 rpm and X8= 25°C	
The predicted removal rate of Congo red (%)	56.52
The experimental removal rate of Congo red	58.17
Error (%)	1.65
GWO: X1 = 20 min, X2 = 30 min, X3 = 170 mg L ⁻¹ , X4 = 10 mL L ⁻¹ , X5 = 3, X6 = 1 M, X7= 30 rpm and X8 = 60°C	
The predicted removal rate of Congo red (%)	53.23
The experimental removal rate of Congo red (%)	51.83
Error (%)	1.4

605

606 3.6. *Comparison of Pinus halepensis Mill. seed extract coagulating performances*
 607 *with ferric chloride (FeCl₃)*

608 For comparative purposes, 50 mg L⁻¹ of Congo red dye were treated with different
 609 amounts of ferric chloride (results not shown), to do so, optimal conditions obtained
 610 earlier were taken into consideration. Using the Imhoff cones method, the quantity of
 611 wet sludge generated by the two coagulants (FeCl₃ and PhsEXT) was also studied.
 612 According to **Table 6**, PhsEXT and FeCl₃ demonstrated nearly identical removal rates
 613 (81.22 % and 83.78 %, respectively); FeCl₃ generated higher sludge quantity (about
 614 18 mL more) comparing to PhsEXT. Similar results have been reported by (Choudhary
 615 et al., 2019; Kristianto et al., 2019). Organic polymers typically generate less sludge
 616 than chemical coagulants since they don't contribute in adding weight to the water or
 617 react chemically with some other ions to form precipitates. Thus, the sludge formed by
 618 PhsEXT was volume-reduced and compressed. This can also be attributed to the

619 difference between flocs formed when FeCl_3 and the biocoagulant were used (Dalvand
 620 et al., 2016). This shows that substituting chemical coagulants with natural ones may
 621 reduce sludge handling costs. The use of conventional coagulants generates a
 622 massive volume of non-biodegradable sludge. This sludge is often disposed of in
 623 conventional landfills, as there is currently no rule tightly regulating the management
 624 of aluminum and iron in sludge. It has been demonstrated that the use of
 625 biocoagulants/biofloculants significantly reduces the amount of sludge generated
 626 during treatment operations by up to 30% (Kurniawan et al., 2020). Additionally, since
 627 all *Pinus halepensis* byproducts are biodegradable organics, the sludge may be utilized
 628 as a fertilizer as long as no heavy metals are present in the treated water. The present
 629 findings demonstrate the great efficiency of PhsEXT as a natural coagulant substitute
 630 for traditional ones.

631 **Table 6** Comparison of *Pinus halepensis* Mill. seeds based biocoagulant with ferric
 632 chloride (FeCl_3) in coagulating Congo red. (Mean \pm SD, n = 3)

Coagulant	Coagulant dosage (mL L ⁻¹)	% Dye removal	Sludge volume (mL L ⁻¹)
PhsEXT	10	81.2 \pm 3.7	28 \pm 1
FeCl₃	10	83.8 \pm 3.6	46 \pm 1

633

634

635 4. Conclusion

636 The findings of the current investigation show that PhsEXT has significant potential
 637 as a natural coagulant and may thus be considered an interesting contribution in the
 638 field of natural resources development. At pH = 3, optimum performance was achieved
 639 with a biocoagulant dosage of 10 mL L⁻¹ and an initial Congo red concentration of 50
 640 mg L⁻¹, yielding 81% of dye removal. Under acidic conditions, PhsEXT performed
 641 similarly to ferric chloride, yet produced less sludge and larger flocs. Seed's proximate
 642 composition and FTIR analysis corroborate the theory that charge neutralization
 643 (proteins— SO_3^{2-} groups of the dye) is the main mechanism occurring in this study. Due
 644 to the very high statistical coefficients ($R = 0.9998$, $R^2 = 0.9995$, and $R^2 \text{ adj} = 0.9995$)

645 and significantly lower statistical errors (RMSE = 0.5813, MSE = 0.3379, EPM =
646 0.9808, ESP = 0.9677, and MAE = 0.2382), the SVM_GWO model exhibited
647 remarkable accuracy. In addition, the efficacy of the model was demonstrated using a
648 variety of methodologies, including test interpolation and residual analysis. This
649 highlights the advantages of combining SVM with GWO.

650 The outcomes of this work indicate that *Pinus halepensis* seeds as a biocoagulant
651 has a promising future in the wastewater treatment field and may be a good alternative
652 to chemical coagulants/flocculants in order to reduce environmental pollution and
653 health hazards associated with their usage.

654
655
656

657 **Acknowledgements**

658 The authors would like to thank everyone who assisted them with this project.

659

660 **Funding**

661 The study is not dependent on any particular funding source in any form.

662

663 **Compliance with Ethical Standards**

664 The submitted work is an original article. It does not contain any human/animal
665 experiments. The paper is original, has not been submitted to another journal for
666 simultaneous review, and has not been published in any form or language elsewhere.

667 **Data availability statement**

668 The authors certify that the data backing the study's conclusions are included in the
669 publication [and/or] its supplemental materials.

670

671 **Competing interests**

672 The authors state that they do not have any conflicting interests.

673

674

675

676

677

678

679

680

681

682

683 **References**

- 684
- 685 Abidin, Z.Z., Ismail, N., Yunus, R., Ahamad, I., Idris, A., 2011. A preliminary study on
686 *Jatropha curcas* as coagulant in wastewater treatment. *Environ. Technol.* 32, 971–977.
- 687 Adenan, N.H., Lim, Y., Ting, A., 2022. Removal of triphenylmethane dyes by
688 *Streptomyces bacillaris*: A study on decolorization, enzymatic reactions and toxicity of
689 treated dye solutions. *J. Environ. Manage.* 318, 115520.
690 <https://doi.org/10.1016/j.jenvman.2022.115520>
- 691 Adnan, O., Abidin, Z.Z., Idris, A., Kamarudin, S., Al-Qubaisi, M.S., 2017. A novel
692 biocoagulant agent from mushroom chitosan as water and wastewater therapy.
693 *Environ. Sci. Pollut. Res.* 24, 20104–20112.
- 694 Ali, S.S., Al-Tohamy, R., Mahmoud, Y.A.-G., Kornaros, M., Sun, S., Sun, J., 2022.
695 Recent advances in the life cycle assessment of biodiesel production linked to azo dye
696 degradation using yeast symbionts of termite guts: A critical review. *Energy Rep.* 8,
697 7557–7581.
- 698 Al-Ismail, K., Al-Assoly, N., Saleh, M., 2018. Extraction and functional characterization
699 of isolated proteins from Aleppo pine seeds (*Pinus halepensis* Mill.). *J. Food Meas.*
700 *Charact.* 12, 386–394.
- 701 Alnawajha, M.M., Kurniawan, S.B., Imron, M.F., Abdullah, S.R.S., Hasan, H.A.,
702 Othman, A.R., 2022. Plant-based coagulants/flocculants: characteristics,
703 mechanisms, and possible utilization in treating aquaculture effluent and benefiting
704 from the recovered nutrients. *Environ. Sci. Pollut. Res.* 1–24.
- 705 Amran, A.H., Zaidi, N.S., Syafiuddin, A., Zhan, L.Z., Bahrodin, M.B., Mehmood, M.A.,
706 Boopathy, R., 2021. Potential of carica papaya seed-derived bio-coagulant to remove
707 turbidity from polluted water assessed through experimental and modeling-based
708 study. *Appl. Sci.* 11, 5715.
- 709 Araújo, B., Romao, L., Doumer, M., Mangrich, A., 2016. Evaluation of the interactions
710 between chitosan and humics in media for the controlled release of nitrogen fertilizer.
711 *J. Environ. Manage.* 190, 122–131. <https://doi.org/10.1016/j.jenvman.2016.12.059>
- 712 Ávila, C., Cañas, R.A., de la Torre, F.N., Pascual, M.B., Castro-Rodríguez, V., Cantón,
713 F.R., Cánovas, F.M., 2022. Functional Genomics of Mediterranean Pines, in: *The Pine*
714 *Genomes*. Springer, pp. 193–218.
- 715 Aziz, H.A., Ramli, S.F., 2017. Settling velocity of sludge in coagulation flocculation
716 treatment of leachate using ferric chloride and chitosan. Presented at the AIP
717 Conference Proceedings, AIP Publishing LLC, p. 040028.
- 718 Bahrodin, M.B., Zaidi, N.S., Hussein, N., Sillanpää, M., Prasetyo, D.D., Syafiuddin, A.,
719 2021. Recent advances on coagulation-based treatment of wastewater: transition from
720 chemical to natural coagulant. *Curr. Pollut. Rep.* 7, 379–391.

721

- 722 Baptista, A.T.A., Silva, M.O., Gomes, R.G., Bergamasco, R., Vieira, M.F., Vieira,
723 A.M.S., 2017. Protein fractionation of seeds of *Moringa oleifera* Lam and its application
724 in superficial water treatment. *Sep. Purif. Technol.* 180, 114–124.
- 725 Bargagli Stoffi, F.J., Cevolani, G., Gnecco, G., 2022. Simple Models in Complex
726 Worlds: Occam's Razor and Statistical Learning Theory. *Minds Mach.* 32, 13–42.
- 727 Bello-Rodríguez, V., Cubas, J., Fernández, Á.B., Aguilar, M.J.D.A., González-
728 Mancebo, J.M., 2020. Expansion dynamics of introduced *Pinus halepensis* Miller
729 plantations in an oceanic island (La Gomera, Canary Islands). *For. Ecol. Manag.* 474,
730 118374.
- 731 Beltrán, J., Sánchez-Martín, J., Delgado-Regalado, A., 2009. Removal of Carmine
732 Indigo Dye with *Moringa oleifera* Seed Extract. *Ind. Eng. Chem. Res.* 48, 6512–6520.
733 <https://doi.org/10.1021/ie9004833>
- 734 Benimam, H., Si-Moussa, C., Laidi, M., Hanini, S., 2020. Modeling the activity
735 coefficient at infinite dilution of water in ionic liquids using artificial neural networks and
736 support vector machines. *Neural Comput. Appl.* 32. [https://doi.org/10.1007/s00521-
737 019-04356-w](https://doi.org/10.1007/s00521-019-04356-w)
- 738 Bouchelkia, N., Tahraoui, H., Amrane, A., Belkacemi, H., Bollinger, J.-C., Bouzaza, A.,
739 Zoukel, A., Zhang, J., Mouni, L., 2022. Jujube stones based highly efficient activated
740 carbon for methylene blue adsorption: kinetics and isotherms modeling,
741 thermodynamics and mechanism study, optimization via Response surface
742 methodology and machine learning approaches. *Process Saf. Environ. Prot.* 170, 513–
743 535. <https://doi.org/10.1016/j.psep.2022.12.028>
- 744 Bouselma, A., Abdessemed, D., Tahraoui, H., Amrane, A., 2021. Artificial intelligence
745 and mathematical modelling of the drying kinetics of pre-treated whole apricots. *Kem.*
746 *U Ind.* 70, 651–667.
- 747 Chethana, M., Sorokhaibam, L.G., Bhandari, V.M., Raja, S., Ranade, V.V., 2016.
748 Green approach to dye wastewater treatment using biocoagulants. *ACS Sustain.*
749 *Chem. Eng.* 4, 2495–2507.
- 750 Chua, S.-C., Malek, M.A., Chong, F.-K., Sujarwo, W., Ho, Y.-C., 2019. Red lentil (*Lens*
751 *culinaris*) extract as a novel natural coagulant for turbidity reduction: An evaluation,
752 characterization and performance optimization study. *Water* 11, 1686.
- 753 Colombo, M., 2017. Regularity results for very degenerate elliptic equations, in: *Flows*
754 *of Non-Smooth Vector Fields and Degenerate Elliptic Equations*. Springer, pp. 119–
755 157.
- 756 Crini, G., Torri, G., Lichtfouse, E., Kyzas, G.Z., Wilson, L.D., Morin-Crini, N., 2019. Dye
757 removal by biosorption using cross-linked chitosan-based hydrogels. *Environ. Chem.*
758 *Lett.* 17, 1645–1666.
- 759 Dalvand, A., Gholibegloo, E., Ganjali, M.R., Golchinpoor, N., Khazaei, M., Kamani, H.,
760 Hosseini, S.S., Mahvi, A.H., 2016. Comparison of *Moringa stenopetala* seed extract as
761 a clean coagulant with Alum and *Moringa stenopetala*-Alum hybrid coagulant to

762 remove direct dye from Textile Wastewater. *Environ. Sci. Pollut. Res.* 23, 16396–
763 16405.

764 Dasgupta, J., Sikder, J., Chakraborty, S., Curcio, S., Drioli, E., 2015. Remediation of
765 textile effluents by membrane based treatment techniques: a state of the art review. *J.*
766 *Environ. Manage.* 147, 55–72.

767 Daverey, A., Tiwari, N., Dutta, K., 2019. Utilization of extracts of *Musa paradisica*
768 (banana) peels and *Dolichos lablab* (Indian bean) seeds as low-cost natural coagulants
769 for turbidity removal from water. *Environ. Sci. Pollut. Res.* 26, 34177–34183.

770 Domínguez, J.R., Beltrán de Heredia, J., González, T., Sanchez-Lavado, F., 2005.
771 Evaluation of ferric chloride as a coagulant for cork processing wastewaters. Influence
772 of the operating conditions on the removal of organic matter and settleability
773 parameters. *Ind. Eng. Chem. Res.* 44, 6539–6548.

774 Dzedziński, M., Kobus-Cisowska, J., Stachowiak, B., 2021. *Pinus* species as
775 prospective reserves of bioactive compounds with potential use in functional food—
776 Current state of knowledge. *Plants* 10, 1306.

777 El-Din, G., Amer, A., Malsh, G., Hussein, M., 2017. Study on the use of banana peels
778 for oil spill removal. *Alex. Eng. J.* 57. <https://doi.org/10.1016/j.aej.2017.05.020>

779 Ghodke, P., Sharma, A., Pandey, J., Chen, W.-H., Patel, A., Veeramuthu, A., 2021.
780 Pyrolysis of sewage sludge for sustainable biofuels and value-added biochar
781 production. *J. Environ. Manage.* 298, 113450.
782 <https://doi.org/10.1016/j.jenvman.2021.113450>

783 Hadadi, A., Imessaoudene, A., Bollinger, J.-C., Assadi, A.A., Amrane, A., Mouni, L.,
784 2022a. Comparison of Four Plant-Based Bio-Coagulants Performances against Alum
785 and Ferric Chloride in the Turbidity Improvement of Bentonite Synthetic Water. *Water*
786 14, 3324.

787 Hadadi, A., Imessaoudene, A., Bollinger, J.-C., Cheikh, S., Assadi, A.A., Amrane, A.,
788 Kebir, M., Mouni, L., 2022b. Parametrical Study for the Effective Removal of Mordant
789 Black 11 from Synthetic Solutions: *Moringa oleifera* Seeds' Extracts Versus Alum.
790 *Water* 14, 4109. <https://doi.org/10.3390/w14244109>

791 Han, G., Du, Y., Huang, Y., Wang, W., Su, S., Liu, B., 2022. Study on the removal of
792 hazardous Congo red from aqueous solutions by chelation flocculation and
793 precipitation flotation process. *Chemosphere* 289, 133109.

794 Hussain, G., Haydar, S., 2019. Exploring potential of pearl millet (*Pennisetum*
795 *glaucum*) and black-eyed pea (*Vigna unguiculata* subsp. *unguiculata*) as bio-
796 coagulants for water treatment. *Desalination Water Treat* 143, 184–191.

797 Imessaoudene, A., Cheikh, S., Bollinger, J.-C., Belkhiri, L., Tiri, A., Bouzaza, A., El
798 Jery, A., Assadi, A., Amrane, A., Mouni, L., 2022. Zeolite Waste Characterization and
799 Use as Low-Cost, Ecofriendly, and Sustainable Material for Malachite Green and
800 Methylene Blue Dyes Removal: Box–Behnken Design, Kinetics, and Thermodynamics.
801 *Appl. Sci.* 12, 7587. <https://doi.org/10.3390/app12157587>

802 Kapse, G., Samadder, S., 2021. Moringa oleifera seed defatted press cake based
803 biocoagulant for the treatment of coal beneficiation plant effluent. *J. Environ. Manage.*
804 296, 113202.

805 Katheresan, V., Kansedo, J., Lau, S.Y., 2018. Efficiency of various recent wastewater
806 dye removal methods: A review. *J. Environ. Chem. Eng.* 6, 4676–4697.

807 Kielkopf, C.L., Bauer, W., Urbatsch, I.L., 2020. Bradford assay for determining protein
808 concentration. *Cold Spring Harb. Protoc.* 2020, pdb. prot102269.

809 Kristianto, H., Rahman, H., Prasetyo, S., Sugih, A.K., 2019. Removal of Congo red
810 aqueous solution using *Leucaena leucocephala* seed's extract as natural coagulant.
811 *Appl. Water Sci.* 9, 1–7.

812 Kristianto, H., Verren, L., Prasetyo, S., Sugih, A.K., 2021. Comparison of FeCl₃ and
813 leucaena seeds FeCl₃ extract coagulation performance to treat synthetic Congo red
814 wastewater. Presented at the AIP Conf. Proc., AIP Publishing LLC, p. 040003.
815 <https://doi.org/10.1063/5.0062181>

816 Lapointe, M., Barbeau, B., 2017. Dual starch–polyacrylamide polymer system for
817 improved flocculation. *Water Res.* 124, 202–209.

818 Liu, Y., Li, C., Bao, J., Wang, X., Yu, W., Shao, L., 2022. Degradation of azo dyes with
819 different functional groups in simulated wastewater by electrocoagulation. *Water* 14,
820 123.

821 Madrona, G.S., Serpelloni, G.B., Salcedo Vieira, A.M., Nishi, L., Cardoso, K.C.,
822 Bergamasco, R., 2010. Study of the effect of saline solution on the extraction of the
823 *Moringa oleifera* seed's active component for water treatment. *Water. Air. Soil Pollut.*
824 211, 409–415.

825 Manholer, D.D., de Souza, M.T.F., Ambrosio, E., Freitas, T.K.F. de S., Geraldino,
826 H.C.L., Garcia, J.C., 2019. Coagulation/flocculation of textile effluent using a natural
827 coagulant extracted from *Dillenia indica*. *Water Sci. Technol.* 80, 979–988.

828 Megersa, M., Gach, W., Beyene, A., Ambelu, A., Triest, L., 2019. Effect of salt solutions
829 on coagulation performance of *Moringa stenopetala* and *Maerua subcordata* for turbid
830 water treatment. *Sep. Purif. Technol.* 221, 319–324.

831 Mirjalili, S., Mirjalili, S.M., Lewis, A., 2014. Grey Wolf Optimizer. *Adv. Eng. Softw.* 69,
832 46–61. <https://doi.org/10.1016/j.advengsoft.2013.12.007>

833 Mishra, A., Yadav, A., Agarwal, M., Rajani, S., 2004. Polyacrylonitrile-grafted *Plantago*
834 *psyllium* mucilage for the removal of suspended and dissolved solids from tannery
835 effluent. *Colloid Polym. Sci.* 282, 300–303.

836 Momeni, M., Kahforoushan, D., Abbasi, F., Ghanbarian, S., 2018. Using
837 Chitosan/CHPATC as coagulant to remove color and turbidity of industrial wastewater:
838 Optimization through RSM design. *J. Environ. Manage.* 211, 347–355.
839 <https://doi.org/10.1016/j.jenvman.2018.01.031>

840 Mouni, L., Belkhiri, L., Bollinger, J.-C., Bouzaza, A., Assadi, A., Tirri, A., Dahmoune,
841 F., Madani, K., Remini, H., 2018. Removal of Methylene Blue from aqueous solutions
842 by adsorption on Kaolin: Kinetic and equilibrium studies. *Appl. Clay Sci.* 153, 38–45.

843 Muniyasamy, A., Sivaporul, G., Gopinath, A., Lakshmanan, R., Altaee, A., Achary, A.,
844 Chellam, P.V., 2020. Process development for the degradation of textile azo dyes
845 (mono-, di-, poly-) by advanced oxidation process-Ozonation: Experimental & partial
846 derivative modelling approach. *J. Environ. Manage.* 265, 110397.
847 <https://doi.org/10.1016/j.jenvman.2020.110397>

848 Nhut, H., Hung, N., Lap, B., Han, L., Tri, T., Bang, N., Hiep, N., Ky, N., 2021. Use of
849 Moringa oleifera seeds powder as bio-coagulants for the surface water treatment. *Int.*
850 *J. Environ. Sci. Technol.* 18, 2173–2180.

851 Pan, J.R., Huang, C., Chen, S., Chung, Y.-C., 1999. Evaluation of a modified chitosan
852 biopolymer for coagulation of colloidal particles. *Colloids Surf. Physicochem. Eng. Asp.*
853 147, 359–364.

854 Pardede, A., Budihardjo, M., Purwono, 2018. The Removal of Turbidity and TSS of the
855 Domestic Wastewater by Coagulation-Flocculation Process Involving Oyster
856 Mushroom as Biocoagulant. *E3S Web Conf.* 31, 05007.
857 <https://doi.org/10.1051/e3sconf/20183105007>

858 Pritchard, M., Craven, T., Mkandawire, T., Edmondson, A., O’neill, J., 2010. A study of
859 the parameters affecting the effectiveness of Moringa oleifera in drinking water
860 purification. *Phys. Chem. Earth Parts ABC* 35, 791–797.

861 Putra, R., Amri, R., Ayu, M., 2020. Turbidity removal of synthetic wastewater using
862 biocoagulants based on protein and tannin. Presented at the AIP Conference
863 Proceedings, AIP Publishing LLC, p. 040028.

864 Radhika, B., Aruna, K., 2022. ELUCIDATING A PATHWAY FOR DEGRADATION OF
865 AZO DYE REACTIVE RED 120 BY BACTERIAL CONSORTIUM. *J. Appl. Biol. Sci.* 16,
866 396–417.

867 Rodrigues, C.S., Madeira, L.M., Boaventura, R.A., 2013. Treatment of textile dye
868 wastewaters using ferrous sulphate in a chemical coagulation/flocculation process.
869 *Environ. Technol.* 34, 719–729.

870 Saldarriaga-Hernández, S., Melchor-Martínez, E., Carrillo Nieves, D., Parra, R., Iqbal,
871 H., 2021. Seasonal characterization and quantification of biomolecules from
872 sargassum collected from Mexican Caribbean coast – A preliminary study as a step
873 forward to blue economy. *J. Environ. Manage.* 298, 113507.
874 <https://doi.org/10.1016/j.jenvman.2021.113507>

875 Shamsnejati, S., Chaibakhsh, N., Pendashteh, A.R., Hayeripour, S., 2015.
876 Mucilaginous seed of *Ocimum basilicum* as a natural coagulant for textile wastewater
877 treatment. *Ind. Crops Prod.* 69, 40–47. <https://doi.org/10.1016/j.indcrop.2015.01.045>

878 Sun, Y., Li, D., Lu, X., Sheng, J., Zheng, X., Xiao, X., 2021. Flocculation of combined
879 contaminants of dye and heavy metal by nano-chitosan flocculants. *J. Environ.*
880 *Manage.* 299, 113589. <https://doi.org/10.1016/j.jenvman.2021.113589>

- 881 Šuvalija, S., Serdarević, A., Džubur, A., Lazović, N., 2022. Biocoagulants and
882 Biofloculants in Water and Wastewater Treatment Technology. Presented at the
883 International Conference “New Technologies, Development and Applications,”
884 Springer, pp. 882–889.
- 885 Suykens, J., Van Gestel, T., De Brabanter, J., De Moor, B., Vandewalle, J., 2002. Least
886 squares support vector machines, World Scientific Publishing, Singapore.
- 887 Szygula, A., Guibal, E., Palacín, M., Ruiz, M., Sastre, A., 2009. Removal of an anionic
888 dye (Acid Blue 92) by coagulation–flocculation using chitosan. *J. Environ. Manage.* 90,
889 2979–86. <https://doi.org/10.1016/j.jenvman.2009.04.002>
- 890 Tahraoui, H., Amrane, A., Belhadj, A.-E., Zhang, J., 2022a. Modeling the organic
891 matter of water using the decision tree coupled with bootstrap aggregated and least-
892 squares boosting. *Environ. Technol. Innov.* 27, 102419.
893 <https://doi.org/10.1016/j.eti.2022.102419>
- 894 Tahraoui, H., Belhadj, A.-E., Amrane, A., Houssein, E.H., 2022b. Predicting the
895 concentration of sulfate using machine learning methods. *Earth Sci. Inform.* 1–22.
- 896 Tahraoui, H., Belhadj, A.-E., Hamitouche, A., 2020. Prediction of the Bicarbonate
897 Amount in Drinking Water in the Region of Médéa Using Artificial Neural Network
898 Modelling. *Predviđanje količine bikarbonata u pitkoj vodi regije Médéa modeliranjem*
899 *umjetnom neuronskom mrežom. Kem. U Ind.* 69, 595–602.
900 <https://doi.org/10.15255/KUI.2020.002>
- 901 Tahraoui, H., Belhadj, A.-E., Hamitouche, A., Bouhedda, M., Amrane, A., 2021a.
902 Predicting the concentration of sulfate (SO₄²⁻) in drinking water using artificial neural
903 networks: a case study: Médéa-Algeria. *DESALINATION WATER Treat.* 217.
904 <https://doi.org/10.5004/dwt.2021.26813>
- 905 Tahraoui, H., Belhadj, A.-E., Moula, N., Bouranene, S., Amrane, A., 2021b.
906 Optimisation and prediction of the coagulant dose for the elimination of organic
907 micropollutants based on turbidity. *Kem. U Ind.* 70, 675–691.
- 908 Tahraoui, H., Belhadj, A.-E., Triki, Z., Boudella, N., Seder, S., Amrane, A., Zhang, J.,
909 Moula, N., Tifoura, A., Ferhat, R., Bousselma, A., Mihoubi, N., 2022c. Mixed
910 Coagulant-flocculant Optimization for Pharmaceutical Effluent Pretreatment Using
911 Response Surface Methodology and Gaussian Process Regression. *Process Saf.*
912 *Environ. Prot.* 169. <https://doi.org/10.1016/j.psep.2022.11.045>
- 913 Teh, C.Y., Wu, T.Y., Juan, J.C., 2014. Potential use of rice starch in coagulation–
914 flocculation process of agro-industrial wastewater: treatment performance and flocs
915 characterization. *Ecol. Eng.* 71, 509–519.
- 916 Tie, J., Jiang, M., Li, H., Zhang, S., Zhang, X., 2015a. A comparison between *Moringa*
917 *oleifera* seed presscake extract and polyaluminum chloride in the removal of direct
918 black 19 from synthetic wastewater. *Ind. Crops Prod.* 74, 530–534.
- 919 Tie, J., Li, P., Xu, Z., Zhou, Y., Li, C., Zhang, X., 2015b. Removal of Congo red from
920 aqueous solution using *Moringa oleifera* seed cake as natural coagulant. *Desalination*
921 *Water Treat.* 54, 2817–2824.

922 Tukan, S., Al-Ismael, K., Ajo, R., Al-Dabbas, M., 2013. Seeds and seed oil compositions
923 of Aleppo pine (*Pinus halepensis* Mill.) grown in Jordan. *Riv Ital Delle Sostanze Grasse*
924 90, 87–93.

925 Vapnik, V., Golowich, S., Smola, A., 1996. Support vector method for function
926 approximation, regression estimation and signal processing. *Adv. Neural Inf. Process.*
927 *Syst.* 9.

928 Vicente, C., Silva, J.R., Santos, A.D., Quinta-Ferreira, R.M., Castro, L.M., 2022.
929 Combined Electrocoagulation and Physicochemical Treatment of Cork Boiling
930 Wastewater. *Sustainability* 14, 3727.

931 Vijayaraghavan, G., Shanthakumar, S., 2015. Efficacy of *Moringa oleifera* and
932 *Phaseolus vulgaris* (common bean) as coagulants for the removal of Congo red dye
933 from aqueous solution. *J. Mater. Environ. Sci.* 6, 1672–1677.

934 Wang, C., Li, G., Ali, I., Zhang, H., Tian, H., Lu, J., 2022. The Management of Energy
935 Transformation through Laser Charging in WPT for 5G Application: Prediction Model
936 of the In0. 3Ga0. 7As Solar Cell. *Wirel. Commun. Mob. Comput.* 2022.

937 Zaidi, N.S., Ting, W., Loh, Z., Bahrodin, M., Awang, N., Kadier, A., 2022. Assessment
938 and optimization of a natural coagulant (*Musa paradisiaca*) peels for domestic
939 wastewater treatment. *Environ. Toxicol. Manag.* 2, 7–13.
940 <https://doi.org/10.33086/etm.v2i1.2901>

941 Zampeta, C., Bertaki, K., Triantaphyllidou, I.-E., Frontistis, Z., Vayenas, D., 2021.
942 Treatment of real industrial-grade dye solutions and printing ink wastewater using a
943 novel pilot-scale hydrodynamic cavitation reactor. *J. Environ. Manage.* 297, 113301.
944 <https://doi.org/10.1016/j.jenvman.2021.113301>

945 Zhang, X., Ye, P., Wu, Y., 2022. Enhanced technology for sewage sludge advanced
946 dewatering from an engineering practice perspective: A review. *J. Environ. Manage.*
947 321, 115938.

948 Zurina, A.Z., Mohd Fadzli, M., Abdul Ghani, L.A., 2014. Preliminary study of rambutan
949 (*Nephelium lappaceum*) seed as potential biocoagulant for turbidity removal.
950 Presented at the Advanced Materials Research, *Trans Tech Publ*, pp. 96–105.

951

952

953

954

955

956

957

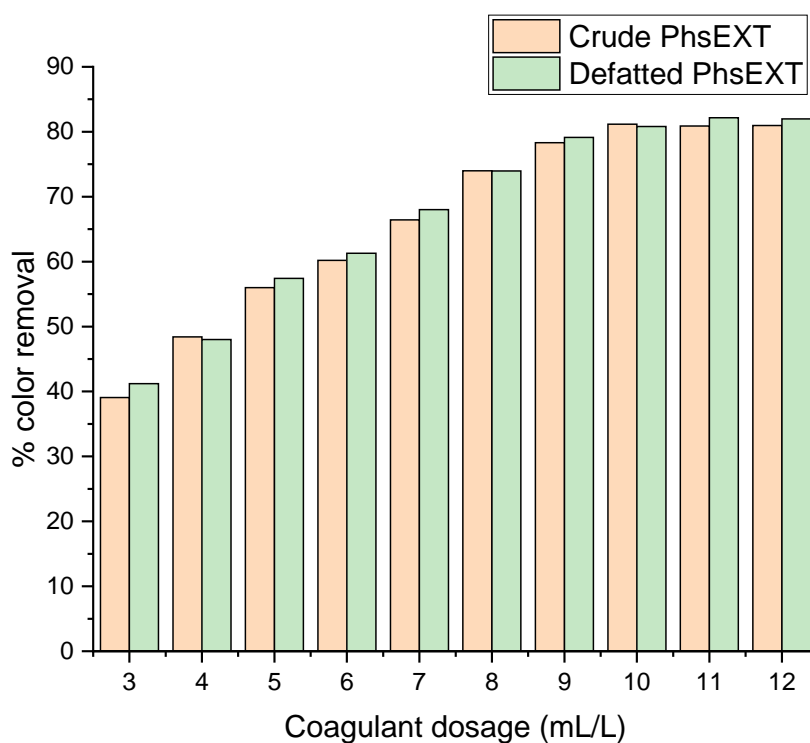
958

959

960 **Supplementary Materials**

961 *1. Influence of defatting Pinus halepensis Mill. seed on coagulation efficiency*

962 the presence of oil might inhibit the extractability of protein and, ultimately, the efficacy
963 of the coagulation process; this phenomenon has been described in a number of prior
964 works (Camacho et al., 2017; Marobhe and Sabai, 2021; Yimer and Dame, 2021). In
965 this regard, a preliminary investigation was conducted on the influence of delipidation
966 on the Aleppo pine seeds coagulation efficiency for the removal of Congo red dye. A
967 hexane extraction was performed according to the methodology given by (Chales et
968 al., 2022). The oil extraction was conducted using a Soxhlet extractor equipment with
969 hexane as the solvent and a solid/solvent ratio of 0.05 g/mL over a period of 3 h (20
970 cycles) to achieve a high oil-removal yield in comparison to other removal approaches
971 (batch) or other solvents (ethanol, ethyl acetate, and acetone). The resulting defatted
972 powder was subjected to the same extraction procedure depicted in the manuscript, 5
973 g were stirred vigorously with 100 mL of 1 M NaCl solution, the coagulation
974 performance of crude and defatted seeds was then evaluated, and the results are
975 presented in the following figure:



976

977 **Fig. 1.** Effect of coagulant dosage on the color removal efficiency of crude and
978 defatted PhsEXT (pH = 3; [NaCl] = 1 M; T = 25°C)

979

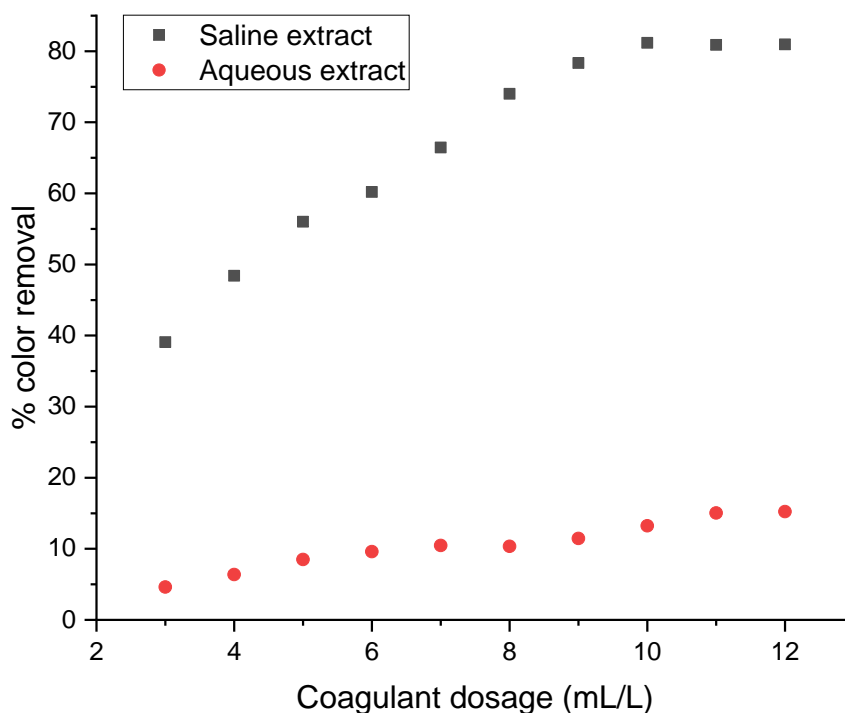
980 As shown in **Fig. 1**, there is a little variation in the removal efficiency of Congo red with
981 seeds that have been defatted, suggesting that this step does not greatly enhance the
982 process and might be skipped, especially because one of our primary objectives was
983 to undertake the dye removal by the novel green coagulant with as few steps as
984 possible to preserve the eco-friendly nature of the investigation. Such results have
985 been reported by (Chales et al., 2022), indeed, the defatting step of *Moringa oleifera*
986 seeds (MOS) did not improve the turbidity removal capacity of seeds' saline extract,
987 but rather reduced the cytotoxicity of the treated water and generated a significant by-
988 product (edible MOS oil).

989 2. *Pinus halepensis* Mill. seed extract (PhsEXT) coagulating agent

990 Concerning the possible influence of carbohydrates on the coagulation
991 performance, a preliminary investigation was carried out in order to confirm or refute
992 this possibility. Indeed, as is well known in the domain of biocoagulation-
993 bioflocculation, natural coagulants are typically made up of carbohydrates and protein,
994 with polysaccharide and amino acids functioning as the building blocks, either through
995 charge neutralization, generally attributable to amino acids, or bridging phenomenon,
996 usually linked to polysaccharide. The above mentioned phenomena are the primary
997 mechanisms that govern biocoagulation-bioflocculation activity (Panwar et al., 2022).

998 A number of studies have reported the involvement of carbohydrates in the
999 coagulation process (Mardarveran and Mohd Mokhtar, 2020) through the bridging
1000 mechanism. Our preliminary investigation involved examining the efficacy of an
1001 aqueous extract of Aleppo pine seeds according to the methodology reported in those
1002 previous studies. The dried *Pinus halepensis* seeds were sieved to a particle size of
1003 0.5 mm. Then, 5 g of the dried raw materials was soaked in 100 ml of distilled water
1004 and stirred vigorously for 30 minutes. The obtained extract was centrifuged and filtered
1005 according to the same methodology depicted in the manuscript and tested on a 50
1006 mg/L Congo red solution, the results are presented in **Fig. 2** (results for saline extract
1007 were incorporated for comparative purposes).

1008



1009

1010 **Fig. 2.** Effect of coagulant dosage of saline and aqueous PHsEXT on the removal of
 1011 Congo red (pH = 3; Congo red concentration = 50 mg/L; [NaCl] = 1 M; T = 25°C)

1012

1013 As can be observed in **Fig. 2**, there is a noticeable difference in the efficacy of
 1014 the two seed extracts. The saline extract significantly outperforms the aqueous one,
 1015 with an elimination rate of 80%, whereas the aqueous extract exhibits negligible Congo
 1016 red removal. As stated in the manuscript, results and discussion section, (3.2.4. *Effect*
 1017 *of NaCl concentration*), the increase in salt concentration promotes a better protein
 1018 extraction through the salting-in mechanism, which refers to the process of increasing
 1019 the ionic strength of a solution to boost solubility of protein leading, ultimately, to a
 1020 dramatical increase in Congo red removal (from 0.1 M to 1 M NaCl).

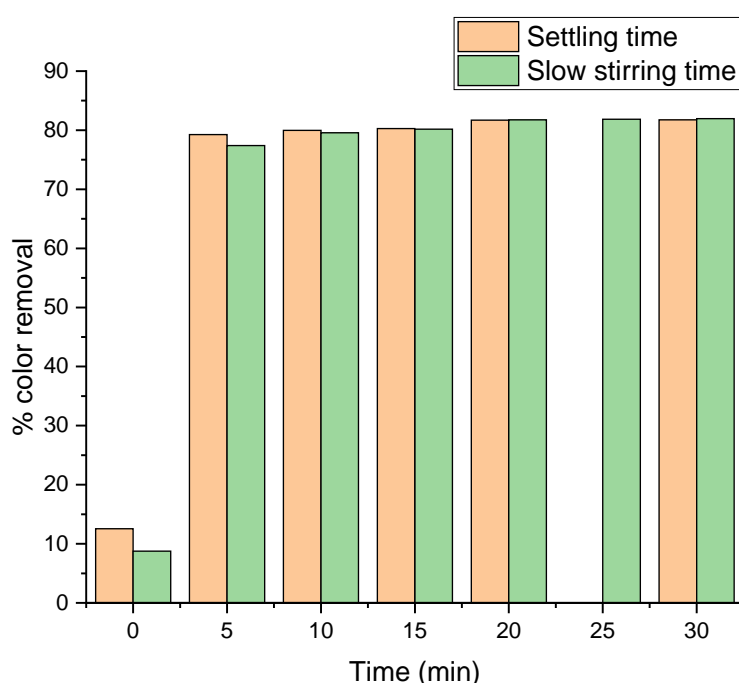
1021 Based on the data presented in **Fig. 2** and the section on the effect of NaCl
 1022 concentration, it is obvious that proteins are the main protagonists in the coagulation
 1023 process in this research.

1024 This theory could also be confirmed by the effect of pH on coagulation efficiency
 1025 (3.2.1. *Effect of initial pH on Congo red removal*), indeed, (Abidin et al., 2011; Bahrodin

1026 et al., 2021) reported that the coagulation mechanism is charge neutralization when
1027 the difference between maximum removal and minimum removal by using different pH
1028 is around 50% or more, which is the case in our investigation. Also, bridging cannot be
1029 considered as a possible mechanism because unlike charge neutralization, bridging is
1030 least affected by pH. however, at lower pH, the polymeric chains responsible for
1031 interparticle bridging will expand and be able to attach to additional pollutants (Momeni
1032 et al., 2018; Zaidi et al., 2022).

1033

1034 3. Effect of slow stirring time and floc settling time on dye removal



1035

1036 **Fig. 3.** Effect of stirring time (flocculation stage) and settling time on dye removal
1037 efficiency.

1038

1039

1040

1041
1042
1043
1044
1045
1046
1047
1048
1049
1050
1051
1052
1053
1054
1055

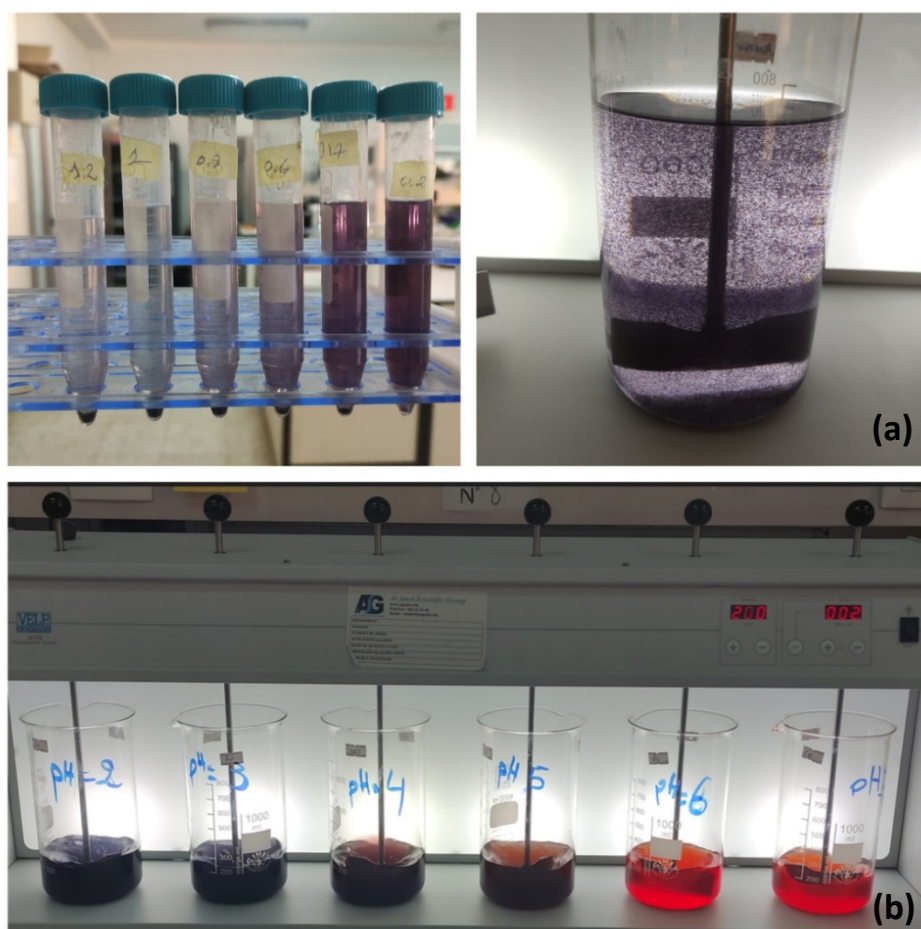


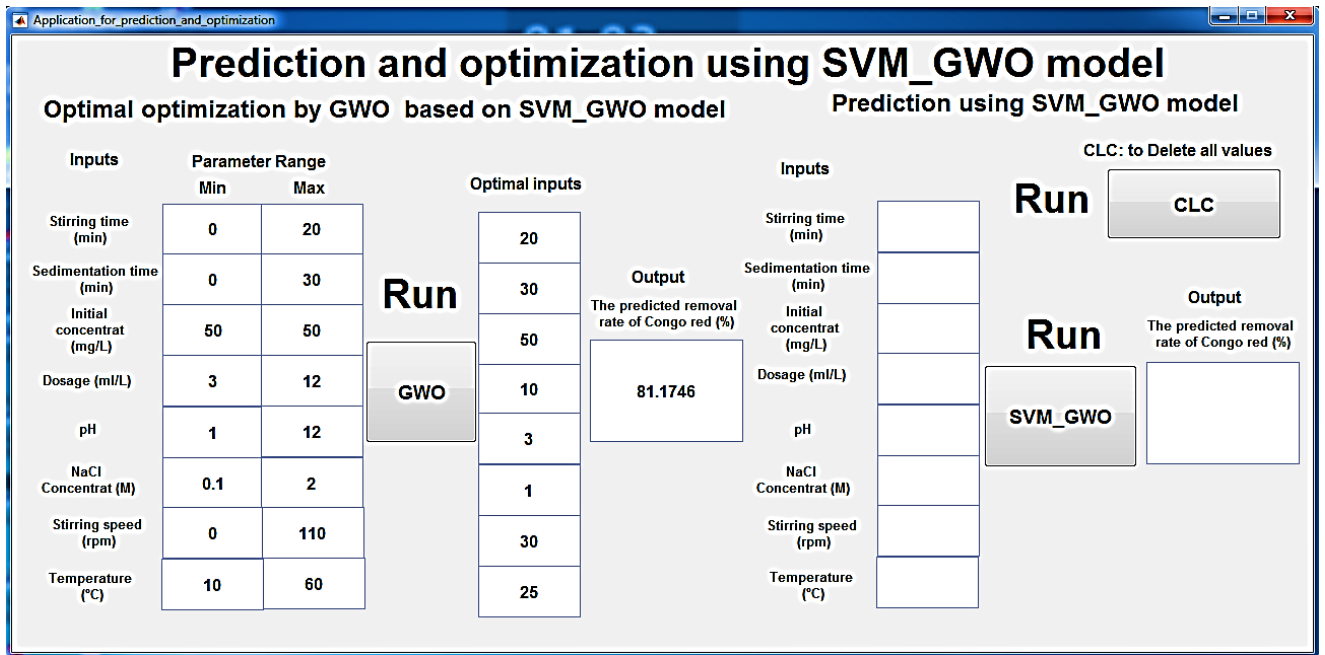
Fig. 4. (a) Representation of the discoloration process after treatment with *PhsEXT*,
(b) Jar-test apparatus used in this study.

1058

4. Interface for optimization and prediction

To provide a simple way to implement the optimization and predict the removal rate of Congo red by biocoagulant, an interface was designed using the MATLAB guide for optimization and prediction (**Fig. 5**). This interface tool has been converted into an executable application under Windows. This powerful direct-to-use application predicts the output by selecting values input by SVM_GWO. In addition, the application also helps to find an optimal solution by GWO.

1066

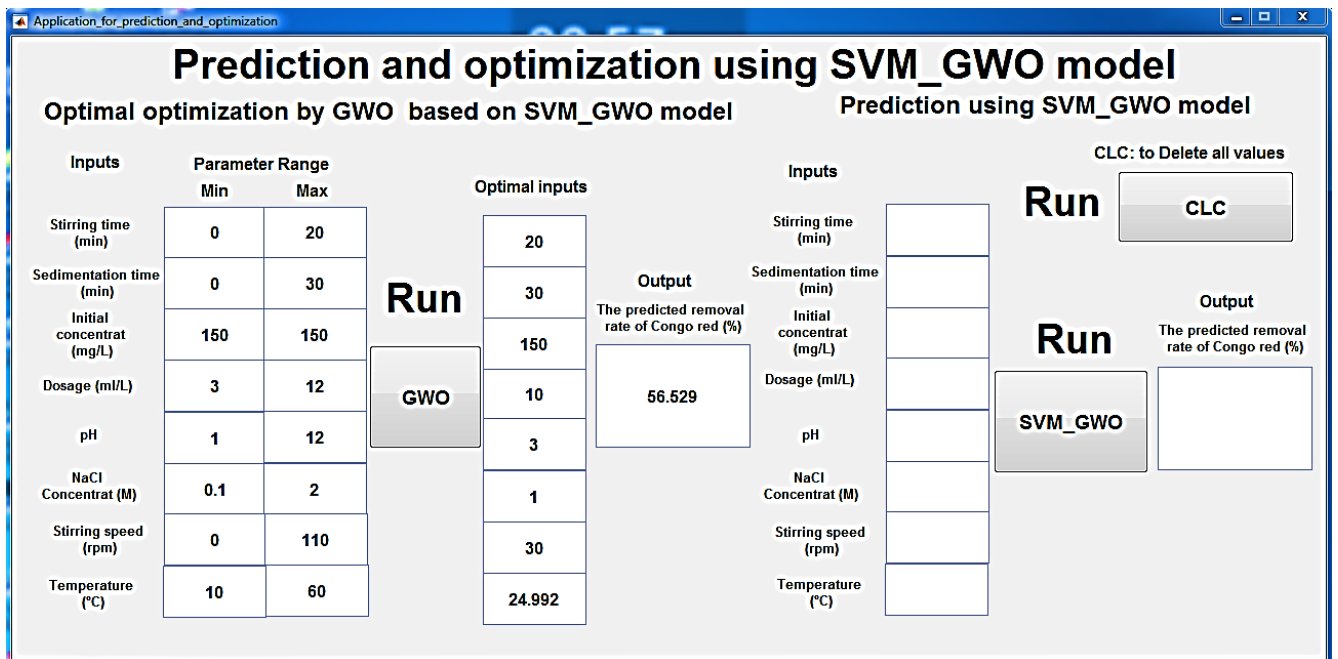


1067

1068

1069

(a)

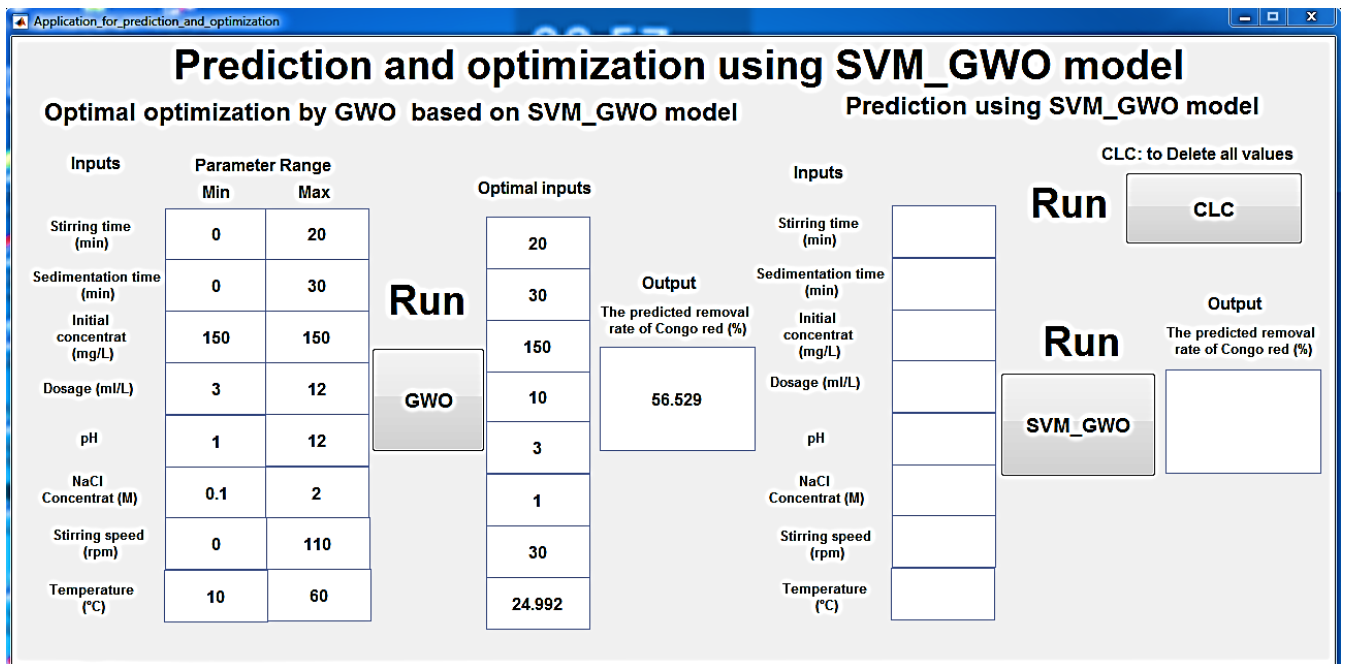


1070

1071

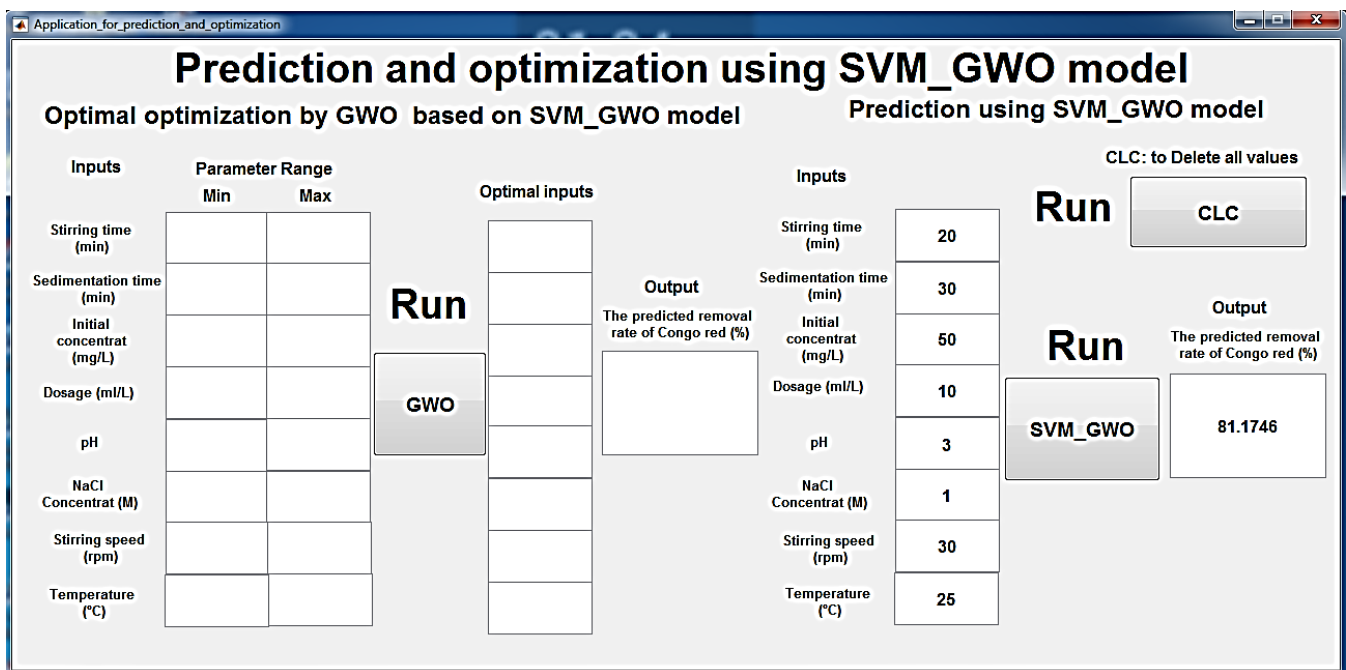
1072

(b)



1073
1074
1075

(c)



1076
1077

(d)

1078 **Fig. 5.** MATLAB Interface: Optimization of optimal using GWO for (a) concentration
1079 50 mg/L, (b) concentration 150 mg/L, (c) concentration 170 mg/L, and (d) prediction
1080 the removal rate of Congo red with SVM_GWO model.

1081
1082
1083

1084 **Supplementary Materials references**

- 1085 Abidin, Z.Z., Ismail, N., Yunus, R., Ahamad, I., Idris, A., 2011. A preliminary study on
1086 *Jatropha curcas* as coagulant in wastewater treatment. *Environ. Technol.* 32,
1087 971–977.
- 1088 Bahrodin, M.B., Zaidi, N.S., Hussein, N., Sillanpää, M., Prasetyo, D.D., Syafiuddin, A.,
1089 2021. Recent advances on coagulation-based treatment of wastewater:
1090 transition from chemical to natural coagulant. *Curr. Pollut. Rep.* 7, 379–391.
- 1091 Camacho, F., Serrão Sousa, V., Bergamasco, R., Teixeira, M., 2017. The use of
1092 *Moringa oleifera* as a natural coagulant in surface water treatment. *Chem. Eng.*
1093 *J.* 313, 226–237. <https://doi.org/10.1016/j.cej.2016.12.031>
- 1094 Chales, G., Tihameri, B., Vicensoto Moreira Milhan, N., Koga Ito, C., Antunes, M., Reis,
1095 A., 2022. Impact of *Moringa oleifera* Seed-Derived Coagulants Processing
1096 Steps on Physicochemical, Residual Organic, and Cytotoxicity Properties of
1097 Treated Water. *Water* 14, 2058. <https://doi.org/10.3390/w14132058>
- 1098 Mardarveran, P., Mohd Mokhtar, N., 2020. Performance of jackfruit (*Artocarpus*
1099 *heterophyllus*) peel coagulant in turbidity reduction under different pH of
1100 wastewater. *Mater. Today Proc.* 46.
1101 <https://doi.org/10.1016/j.matpr.2020.10.248>
- 1102 Marobhe, N., Sabai, S., 2021. Treatment of drinking water for rural households using
1103 *Moringa* seed and solar disinfection. *J. Water Sanit. Hyg. Dev.* 11.
1104 <https://doi.org/10.2166/washdev.2021.253>
- 1105 Momeni, M., Kahfroushan, D., Abbasi, F., Ghanbarian, S., 2018. Using
1106 Chitosan/CHPATC as coagulant to remove color and turbidity of industrial
1107 wastewater: Optimization through RSM design. *J. Environ. Manage.* 211, 347–
1108 355. <https://doi.org/10.1016/j.jenvman.2018.01.031>
- 1109 Panwar, K., Dadhich, I., Dave, M., Sharma, Y., Shaik, N., 2022. Effective Waste Water
1110 Treatment by the Application of Natural Coagulants. *Adv. Mater. Sci. Eng.* 2022,
1111 1–5. <https://doi.org/10.1155/2022/3023200>
- 1112 Yimer, A., Dame, B., 2021. Papaya seed extract as coagulant for potable water
1113 treatment in the case of Tulte River for the community of Yekuset district,
1114 Ethiopia. *Environ. Chall.* 4, 100198. <https://doi.org/10.1016/j.envc.2021.100198>
- 1115 Zaidi, N.S., Ting, W., Loh, Z., Bahrodin, M., Awang, N., Kadier, A., 2022. Assessment
1116 and optimization of a natural coagulant (*Musa paradisiaca*) peels for domestic
1117 wastewater treatment. *Environ. Toxicol. Manag.* 2, 7–13.
1118 <https://doi.org/10.33086/etm.v2i1.2901>

1120

1121

1122